THE SEISMOLOGICAL SOCIETY OF AMERICA
400 Evelyn Ave., Suite 201
Albany, CA 94706-1375
(510) 525-5474; FAX (510) 525-7204
www.seismosoc.org

Bulletin of the Seismological Society of America, Vol. 102, No. 1, pp. 143–168, February 2012, doi: 10.1785/0120110078

An Evaluation of the Applicability of Current Ground-Motion Models to the South and Central American Subduction Zones

by M. C. Arango,* F. O. Strasser, J. J. Bommer, J. M. Cepeda, R. Boroschek, D. A. Hernandez, and H. Tavera

Abstract The applicability of existing ground-motion prediction equations (GMPEs) for subduction-zone earthquakes is an important issue to address in the assessment of the seismic hazard affecting the Peru–Chile and Central American regions. Few predictive equations exist that are derived from local data, and these do not generally meet the quality criteria required for use in modern seismic hazard analyses. This paper investigates the applicability of a set of global and regional subduction ground-motion models to the Peru–Chile and Central American subduction zones, distinguishing between interface and intraslab events, in light of recently compiled ground-motion data from these regions. Strong-motion recordings and associated metadata compiled by Arango, Strasser, Bommer, Boroschek, *et al.* (2011) and Arango, Strasser, Bommer, Hernandez, *et al.* (2011) have been used to assess the performance of the candidate equations following the maximum-likelihood approach of Scherbaum *et al.* (2004) and its extension to normalized intraevent and interevent residual distributions developed by Stafford *et al.* (2008). The results of this study are discussed in terms of the transportability of GMPEs for subduction-zone environments from one region to another, with a view to providing guidance for developing ground-motion logic trees for seismic hazard analysis in these regions.

Online Material: Tables summarizing the statistics for the Scherbaum *et al.* (2004) scoring system.

Introduction

The applicability of existing ground-motion prediction equations (GMPEs) for subduction-zone earthquakes is an important issue to address in the assessment of the seismic hazard affecting the South and Central American regions. Few subduction-zone equations exist that are derived from local data, and these do not generally meet the quality criteria required for use in modern seismic hazard analyses (e.g., Cotton *et al.*, 2006; Bommer *et al.*, 2010). As a result, it has become common practice to use subduction-zone GMPEs derived from global datasets, or even equations for other regions, when performing seismic hazard analyses of the South and Central American regions. The underlying assumption is that broadly similar tectonic regimes produce comparable ground motions and that factors such as careful selection of strong-motion recordings, consistent determination of the associated metadata, and appropriate modeling of the physical processes involved in the generation and propagation of ground motions ultimately have a stronger impact on the predictive capability of GMPEs than does the geographic origin of the data on which they are based. Comparisons with observed data support this assumption in the case of ground motions from shallow crustal events in tectonically active regions (e.g., Bommer, 2006). However, its validity is unclear in the case of subduction-zone ground motions, not least because of the significant differences in terms of physical properties of the source observed from one subduction zone to another. The impact of these differences on the ground motions generated is still poorly understood.

Previous studies investigating the regional variability of ground motions from subduction zones (Atkinson and Boore, 2003; Atkinson and Casey, 2003; Atkinson and Macias, 2009; García and Wald, 2010) and the transportability of subduction-zone GMPEs to regions other than that for which they have been derived (Douglas and Mohais, 2009) found significant differences in ground-motion behavior from one region to another. Until recently, strong-motion recordings from subduction earthquakes perhaps have received less attention than those from crustal events, and such data have been lacking from many regions. This has

*Current address: Arup, 13 Fitzroy Street, London W1T 4BQ, United Kingdom.

prompted the tendency to use models derived from data recorded in different regions from those in which the seismic hazard is being assessed, frequently without questioning the validity of the underlying assumption of similarity among subduction zones in terms of ground motions.

In this study, we investigate the extent to which global and overseas regional GMPEs for subduction-zone earthquakes may be applied to the South and Central American subduction zones in light of recently compiled strong-motion data. This study focuses more particularly on the specific area that includes the subduction zone of Peru–Chile in South America and the Central American segment of subduction that extends from Costa Rica to Guatemala. A suite of global and overseas regional GMPEs for subduction-zone earthquakes are compared against sets of strong-motion recordings and associated metadata compiled for Peru and Chile (Arango, Strasser, Bommer, Boroschek, *et al.*, 2011), as well as for El Salvador, Costa Rica, Nicaragua, and Guatemala (Arango, Strasser, Bommer, Hernandez, *et al.*, 2011). The applicability of the candidate GMPEs is evaluated using the maximum-likelihood approach of Scherbaum *et al.* (2004) and its extension to normalized intra- and interevent model residuals developed by Stafford *et al.* (2008). We note the nomenclature proposed by Al Atik *et al.* (2010), in which the terms "interevent" and "intraevent" are replaced by "between-event" and "within-event," which is clearer and in this context avoids confusion with interface and intraslab as categories of subduction earthquakes. However, we retain the established terminology herein for consistency with the notation used by Stafford *et al.* (2008), which is the methodological basis for this study.

The Scherbaum *et al.* (2004) method and its extension provide a rational and objective framework for assessing the performance of existing GMPEs by examining the statistics of the distributions of the residuals between predictions from the candidate equations and observations, as well as the associated likelihood functions. This method has been successfully applied in several recent studies to examine the suitability of equations for the prediction of ground motions in different regions (e.g., Bindi *et al.*, 2006; Douglas *et al.*, 2006; Drouet *et al.*, 2007; Hintersberger *et al.*, 2007; Stafford *et al.*, 2008; Douglas and Mohais, 2009). The results of the present study are discussed in terms of the transportability of global GMPEs and those from other regions to the South and Central American subduction zones. Regional differences in performance are investigated as a tool to assist in the construction of ground-motion logic trees for seismic hazard analysis in these regions.

Existing Subduction-Zone Models for South and Central America

To the best of our knowledge, there is currently no regional subduction-zone GMPE available for either the Peru–Chile or the Central American region that meets the quality criteria used for the selection of GMPEs in modern seismic hazard analyses (Cotton *et al.*, 2006; Bommer *et al.*, 2010). Nevertheless, a number of Chilean models for peak ground acceleration (PGA) have been proposed in the gray literature and conference papers (e.g., Martín, 1990; Medina, 1998; Saragoni *et al.*, 2004; Ruiz and Saragoni, 2005). In particular, Saragoni *et al.* (2004) and Ruiz and Saragoni (2005) developed predictive equations for both interface and intraslab events using exclusively data recorded by the Chilean strong-motion network. However, this condition limits the number of records used in their regression to 76, which raises doubts about the robustness and adequate constraint of these equations. Ongoing research at the University of Chile (e.g., Contreras, 2009) is investigating the development of new GMPEs for the Chilean region.

Equations for subduction-zone events in Central America have been developed by Alfaro *et al.* (1990), Climent *et al.* (1994), Bommer *et al.* (1996), Schmidt *et al.* (1997), and Cepeda *et al.* (2004). Similar to the Peru–Chile case, early subduction GMPEs for Central America (Alfaro *et al.*, 1990; Bommer *et al.*, 1996; Schmidt *et al.* 1997) were based on very limited strong-motion data (less than 50 records), and these did not account for differences between interface and intraslab events. Furthermore, Climent *et al.* (1994) did not find apparent differences between ground motions from shallow crustal and subduction events in Central America; hence, they developed a generic model for the region using database of 280 records from Central America and Mexico. More recently, Cepeda *et al.* (2004) derived equations that are specific to subduction intraslab events for PGA and 5%-damped pseudospectral acceleration (PSA) at 0.3 and 1.0 s. These were developed by adjusting the magnitude scaling term of the Atkinson and Boore (2003) intraslab model, using data from the 13 January 2001 (M_w 7.7) El Salvador earthquake and associated aftershocks. The characteristics of the subduction-zone models available for the Peru–Chile and Central American regions are summarized in Table 1.

Overview of Global and Overseas Regional Subduction-Zone Models

Although subduction-zone seismicity accounts for about 75% of the seismic moment release at a global scale, only a limited number of GMPEs for subduction-zone environments have been developed to date, compared to the large number of predictive equations available for shallow crustal environments. Table 2 summarizes global and overseas regional ground-motion models for subduction regimes that have been published over the last decade. In addition, it lists the model recently developed by N. A. Abrahamson and coworkers for BC Hydro (2010) using worldwide data and the global model of Atkinson and Boore (2003, 2008), which updated earlier studies by Crouse (1991) and Youngs *et al.* (1997), the latter of which is also included in Table 1 because it is still widely used.

Table 2 also includes regional models for the New Zealand (McVerry *et al.*, 2006), Mexican (García *et al.*,

Table 1
Summary Characteristics of Existing Subduction-Zone GMPEs for the Peru–Chile and Central American Regions

Reference	Region	Y*	C†	N_R‡	M§	$[M]$§	R‖	$[R]$ (km)‖
Alfaro *et al.* (1990)	Guatemala, Nicaragua, and El Salvador	PGA	LH	$s = 20$	M_s	4.1–7.5	R_{epi}	5–27
Climent *et al.* (1994)	Costa Rica, Nicaragua, El Salvador, and Mexico	PGA, PSV	LH	$s + c = 280$	M_w	4.0–8.0	R_{hyp}	5–400
Bommer *et al.* (1996)	El Salvador	PGA, PSV	LH	$s = 36$	M_s	3.7–7.0	R_{hyp}	62–260
Schmidt *et al.* 1997)	Costa Rica	PGA, PSV	LH	$s = 67$	M_w	3.7–7.6	R_{hyp}	6–150
Cepeda *et al.* (2004)	El Salvador	PGA, PSA at 0.30 and 1.0 s	LH	$n = 254$	M_w	2.8–7.7	R_{hyp}	57–190
Ruiz and Saragoni (2005)	Chile	PGA	LH	$t = 41$, $n = 22$	M_s	6.2–7.8	R_{hyp}	36–315

*Predicted ground-motion parameter: PGA, peak ground acceleration; PSA, pseudospectral acceleration; PSV, pseudospectral velocity.
†Horizontal component definition: LH, larger horizontal component.
‡Number of records in underlying dataset: s, generic subduction records; t, interface records; n, intraslab records; c, shallow crustal records.
§Magnitudes: M, magnitude scale in equation; $[M]$, range of magnitudes in dataset.
‖Distance metric in equation, R: R_{hyp}, hypocentral distance; R_{epi}, epicentral distance. $[R]$, range of distance in dataset.

2005; Arroyo *et al.*, 2010), Japanese (Zhao *et al.*, 2006; Kanno *et al.*, 2006), Indo-Burmese (Gupta, 2010), and Taiwanese (Lin and Lee, 2008) subduction zones. The Takahashi *et al.* (2004) model differs only slightly from the Zhao *et al.* (2006) model, so the former model is not listed. We have only considered empirical GMPEs and not those derived using stochastic (e.g., Atkinson and Boore, 1997; Gregor *et al.*, 2002; Atkinson and Macias, 2009) or other types of simulations (e.g., Megawati *et al.*, 2005; Megawati and Pan, 2010). We note at this point that the model of Gupta (2010) is listed here for completeness but not considered any further in this study because we believe this model is very unlikely to be employed for probabilistic seismic hazard analysis (PSHA) in regions other than that for which it was derived.

All the equations listed in Table 2 account for differences in ground motion between subduction interface and intraslab events; however, not all the models provide separate sets of coefficients for interface and intraslab events. In the Youngs *et al.* (1997), McVerry *et al.* (2006), Zhao *et al.* (2006), Lin and Lee (2008), and BC Hydro (2010) models, the difference between interface and intraslab events is accommodated via a simple switch using additive terms in the equation. Only Atkinson and Boore (2003) derived separate sets of coefficients for these two earthquake types; Kanno *et al.* (2006) provided separate coefficients for interface and intraslab events, but they also merged the former with crustal earthquakes. GMPEs specific to intraslab earthquakes have been developed by García *et al.* (2005) and Gupta (2010), and equations for interface earthquakes applicable to sites in the forearc region (i.e., the region between the subduction trench and volcanic front) have been derived by Arroyo *et al.* (2010).

Overview of Calibration Data from South and Central America

The calibration databases from the South and Central America regions have been compiled by Arango, Strasser, Bommer, Boroschek, *et al.* (2011) and Arango, Strasser, Bommer, Hernandez, *et al.* (2011). These include 98 records from Peru and Chile (South American dataset) and 554 records from El Salvador, Costa Rica, Nicaragua, and Guatemala (Central American dataset). We refer the reader to Arango, Strasser, Bommer, Boroschek, *et al.* (2011) and Arango, Strasser, Bommer, Hernandez, *et al.* (2011) for a detailed description of these datasets. The distribution of calibration datasets in magnitude–distance space is presented in Figure 1, highlighting the geographic provenance of the data. This figure clearly shows the complementary nature of the South American (SAM) and Central American (CAM) interface datasets, with the SAM region contributing records from large-to-great magnitude events at close distances and the CAM interface dataset predominantly consisting of more distant recordings from moderate-to-large events. These plots also show that the overlap between the two datasets is greater for the intraslab events, although the average magnitude of the SAM dataset still tends to be higher; the greater depth of these intraslab events results in larger source-to-site distances compared to interface events, with all data located at rupture distances (R_{rup}) greater than 50 km.

While South and Central American recordings have been included in the global databases used to derive the Youngs *et al.* (1997), Atkinson and Boore (2003), and BC Hydro (2010) models, their contribution remains marginal when compared to the entire database. About 20% of the Youngs *et al.* (1997) database corresponds to Peruvian–Chilean recordings from both interface and intraslab events, but this model did not include any data from Central America. Atkinson and Boore (2003) expanded earlier compilations by Crouse *et al.* (1988), Crouse (1991), and Youngs *et al.* (1997) by adding nearly 900 horizontal components, mainly from Japan, Cascadia, and Mexico. They also added 8 components from events in Peru (1970, 1971, and 1974 events) and 18 from the January 2001 event in El Salvador. Overall, the Peru–Chile region contributed 72 interface

Table 2

Summary of Empirical Global and Overseas Regional GMPEs for Subduction-Zone Earthquakes Derived over the Last Decade*

Reference	Region	Y†	C‡	T_{max} (s)§	N_R‖	N_Q#	[M]**	R††	[R]††	[h_{max}]‡‡	Type§§	Site Class‖‖
Youngs *et al.* (1997)	Alaska, Cascadia, Chile, Japan, and the Solomon Islands	PGA, SA	GM	4.0	$t = 181$ $n = 53$	$t = 57$ $n = 26$	$t = 5.0–8.2$ $n = 5.0–7.8$	R_{rup}	$t = 8.5–551$ $n = 45–744$	$t = 50$ $n = 130$	t, n (together)	2###
Atkinson and Boore (2003, 2008)	Alaska, Cascadia, Chile, Japan, Mexico, and Peru##	PGA, PSA	R	3.0	$t = 394$ $n = 761$***	$t = 49$ $n = 30$‡‡‡	$t = 5.5–8.3$ $n = 5.0–7.9$	R_{rup}	$t = 5–420$ $n = 34–575$‖‖‖	$t = 50$ $n = 100$	t, n (separate)	4****
García *et al.* (2005)	Central Mexico	PGA, PGV, PSA,	QM	5.0	$n = 267$	$n = 16$	5.2–7.4	R_{rup}	40–400	$n = 138$	n	1††††
McVerry *et al.* (2006)	New Zealand +66 overseas near-source records	PGA, SA	GM	3.0	535†††	$t = 6$ $n = 19$	5.2–6.8	R_{rup}	30–400	$t = 24$ $n = 149$	t, n (together)	3‡‡‡‡
Zhao *et al.* (2006)	Japan +208 near-source crustal records (Iran and western North America)	PGA, SA	GM	5.0	$t = 1520$ $n = 1725$ $c = 1481$	269§§§	5.0–8.3	R_{rup}	0–300	$t = 50$ $n = 162$	t, n, c (together)	4§§§§
Kanno *et al.* (2006)	Japan + near-source overseas data (western North America and Turkey)	PGA, PGV, PSA	Vect	5.0	$t + c = 3769$ $n = 8150$	$t = 83$ $n = 111$	$t + c = 5.2–8.2$ $n = 5.5–8.0$	R_{rup}	$t + c = 1 - 400$ $n = 30–500$	$t + c = 30$ $n = 180$	$(t + c)$, n (separate)	V_{S30}
Lin and Lee (2008)	Taiwan + near-source overseas data	PGA, SA	GM	5.0	$t = 873$ $n = 3950$	$t = 17$ $n = 37$	$t = 5.3–8.1$ $n = 4.1–6.7$	R_{hyp}	$t = 20–400$ $n = 40–600$	$t = 30$ $n = 161$	t, n (together)	2‖‖‖‖
Arroyo *et al.* (2010)	Forearc region of Mexico (Oaxaca, Guerrero, Michoacan, and Colima)	PGA, PSA	QM	5.0	$t = 418$	$t = 40$	$t = 5.0–8.0$	R_{rup}	$t = 20–400$	$t = 29$	t	1††††
BC Hydro (2010)	Japan, Taiwan, Cascadia, Mexico, Peru, Chile, Alaska, and Solomon Islands	PGA, SA	GM	10	$t = 1378$ $n = 3946$	$t = 46$ $n = 76$	$t = 6.5–8.4$ $n = 5.0–7.9$	R_{rup} R_{hyp}	$t = 5–551$ $n = 34–991$	$t = 50$ $n = 194$	t, n (together)	V_{S30}

(*continued*)

Table 2 (*Continued*)

Reference	Region	Y†	C‡	T_{max} (s)§	N_R‖	N_Q#	[M]**	R††	[R]††	[h_{max}]‡‡	Type§§	Site Class‖‖
Gupta (2010)	Northeast India	PGA, PSA	GM	3.0	$n = 56$	$n = 3$	$n = 6.3$–7.2	R_{rup}	$n = 165$–370	$n = 118$	n	4####

*For completeness, the widely used model of Youngs *et al.* (1997) is also listed.

†PGA, peak ground acceleration; PSA, pseudospectral acceleration; SA, absolute spectral acceleration.

‡GM, geometric mean; QM, quadratic mean; R, randomly chosen; Vect, vectorially resolved component (square root of sum of squares of the two components in the time domain).

§Longest response period.

‖Number of records in dataset: *t*, number of records from interface events; *n*, number of records from intraslab events; *c*, number of records from crustal events.

#Number of earthquakes in dataset: *t*, interface; *n*, intraslab.

**[*M*], range of magnitudes in dataset. Note: magnitude scale M_w is used in all GMPEs listed.

††Distance metric in equation, *R*: R_{rup}, closest distance to the fault plane; R_{hyp}, hypocentral distance. [*R*], range of distance in dataset.

‡‡*t*, maximum depth of interface; *n*, intraslab events in dataset.

§§*t*, *n* (together), both interface (*t*) and intraslab (*n*) are modeled by a single equation; *t, n* (separate), two different equations were developed for interface (*t*) and intraslab (*n*) events; *t, n ,c* (together), the interface (*t*), intraslab (*n*), and crustal (*c*) are modeled by a single equation.

‖‖Site classes in equation.

##Regions contributing interface data.

***The value listed is the number of horizontal components in the interface dataset.

†††The value listed includes both subduction and crustal records; no breakdown of record numbers by source type is given in the publication.

‡‡‡Value listed is the number of interface events in dataset.

§§§No breakdown of event number by source type is given in the publication.

‖‖‖Only data from events up to 300 km used for final regression;

###Only two classes are modeled (generic rock and soil).

****Four site classes (B to E) are modeled following the NEHRP (1997) site classification.

††††Only rock sites (NEHRP B) are modeled.

‡‡‡‡Three site classes are modeled following New Zealand site classification, based on surface geology description, geotechnical properties, V_{S30} values, natural site period (T_0), and depth to bedrock.

§§§§Four site classes are determined based on V_{S30} values and natural period (T_0) of the site.

‖‖‖‖Only two classes are modeled: rock (equivalent to NEHRP site class B and C) and soil (equivalent to NEHRP site class D and E).

####Equation adjusted from AB2003 model (hence it uses the same four NEHRP site classes, B–E).

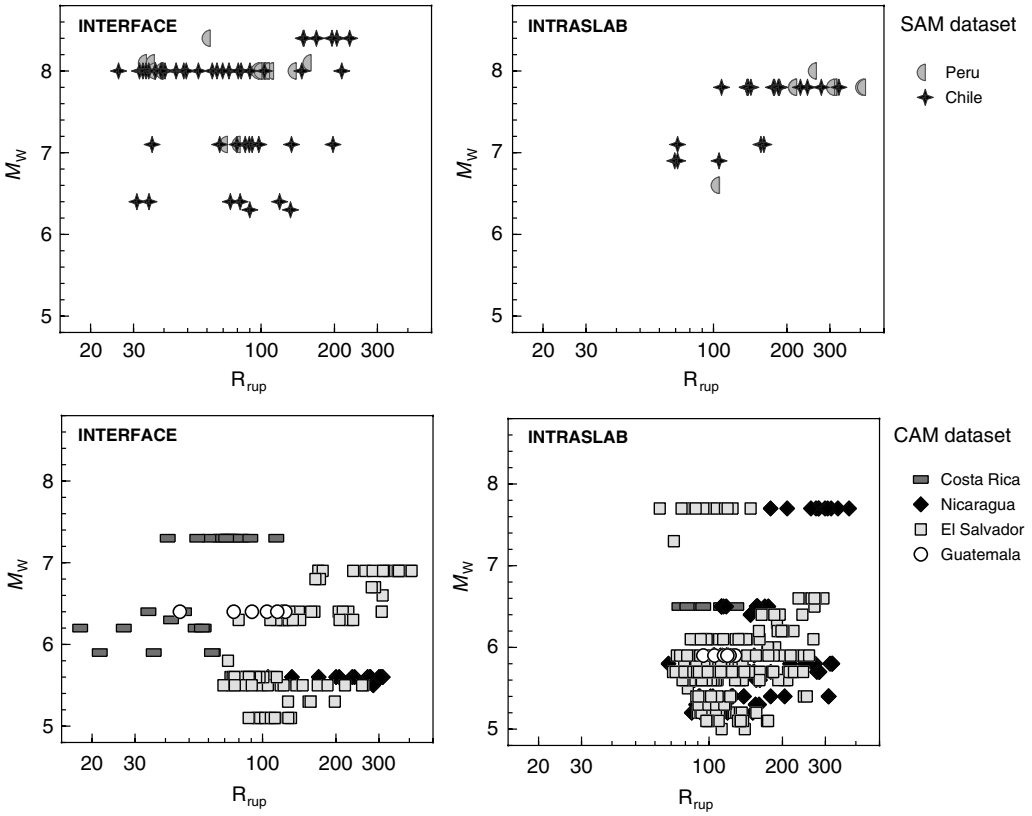

Figure 1. Distribution of the (top) South American (SAM) and (bottom) Central American (CAM) calibration datasets from interface and intraslab earthquakes.

components (about 18%) and 8 intraslab components (about 1%) to the Atkinson and Boore (2003) interface and intraslab datasets, respectively. Central American data represent less than 3% of the Atkinson and Boore (2003) intraslab dataset, and no interface data from this region are include in this model. It is worth noting here that the Youngs *et al.* (1997) and Atkinson and Boore (2003) databases are essentially identical for interface events of magnitudes $M_w \geq 7.5$; but their intraslab databases show very little overlap, with only two recordings in common.

BC Hydro (2010) recently expanded the Atkinson and Boore (2003) database to create a global database of 5324 subduction records, of which about 90% are from Japan and Taiwan. BC Hydro (2010) also added data recorded during the Peruvian–Chilean events on 23 June 2001 (4 records), 15 August 2007 (13 records), and 13 June 2005 (2 records) that had not been included in the earlier study, in addition to 15 more records from El Salvador. Despite the considerable growth of the global subduction database, SAM and CAM data only constitute less than 2% of the BC Hydro (2010) dataset. Presently, more than 30 recordings from the 27 February 2010 (M_w 8.8) Chilean earthquake exist that could be used to develop new subduction-zone models but which were recorded after the databases used in the present study had been compiled.

Overview of Models Tested for Applicability

A set of equations was selected using the preselection criteria of ground-motion models proposed by Cotton *et al.* (2006) and Bommer *et al.* (2010), based on the collection of subduction models presented in Tables 1 and 2. However, we note that these criteria, which were developed for active crustal regions, need to be relaxed slightly when considering subduction regimes for which the number of available GMPEs is relatively small. Most of the existing local models for South and Central America have been excluded from the present analysis, the notable exception being Cepeda *et al.* (2004, hereafter C2004), which is viewed as the only regional model that may be given serious consideration for application in PSHA, as it was specifically derived for intraslab events and provides predictions for two response spectral ordinates, as well as PGA. In particular, the PGA models for the Chilean region and early equations for Central America were rejected on the basis of the limited nature of the datasets from which such models were derived and, in some instances, due to the inappropriateness of their formulations that do not distinguish between subduction source types or even between crustal and subduction regimes (e.g., Climent *et al.*, 1994).

In terms of overseas models, the selected GMPEs include the global models of Youngs *et al.* (1997, hereafter Y1997), Atkinson and Boore (2003, hereafter AB2003) and BC Hydro

(2010, hereafter BC2010), as well as the regional models of García *et al.* (2005, hereafter G2005), McVerry *et al.* (2006, hereafter Mc2006), Zhao *et al.* (2006, hereafter Z2006), Lin and Lee (2008, hereafter LL2008) and Arroyo *et al.* (2010, hereafter AR2010). Although the Y1997 and AB2003 models can be considered as being superseded by the BC2010 global model, the database used to derive the latter is mainly controlled by data from Japan and Taiwan, so all three models have been included in view of the varying importance of South and Central American data in their underlying databases. The functional forms of these three models also differ; hence, their predictions are expected to be different for certain magnitude–distance ranges. The Kanno *et al.* (2006) model was not included in the testing because it was considered redundant to include two Japanese models, and the Z2006 model presents advantages for implementation in a logic-tree framework for PSHA. While the Kanno *et al.* (2006) model uses an unconventional definition for the horizontal component of motion (square root of the sum of squares of the two components in the time domain), the Z2006 model uses the more common geometric mean. Finally, the Gupta (2010) model was not selected for the analysis because it is actually an adjustment of the AB2003 intraslab equation, based on only 37 records at $R_{rup} > 150$ km.

To enable a meaningful comparison between the selected models, differences in terms of parameters definitions, such as horizontal component of motion, magnitude scale, and distance metric, have to be adjusted (e.g., Bommer *et al.*, 2005). The candidate models all use moment magnitude (M_w) and adopt the rupture distance (R_{rup}) as the distance metric, except for the LL2008 and BC2010 intraslab equations, which use the hypocentral distance (R_{hyp}). When making comparisons with the recorded data, issues associated with parameter compatibility in terms of distance metric are irrelevant because both rupture and hypocentral distance estimates are included in the metadata associated with the calibration datasets. Adjustments to account for the different horizontal component definitions of motion are made using the correlations derived by Beyer and Bommer (2006), adopting the geometric mean of motion as the reference definition. We note here that these correlations were derived for crustal motions, and their applicability to the horizontal components of subduction-zone motions has not been confirmed.

As shown in Table 2, the candidate equations all consider different site classification schemes; however, all schemes employed can be translated to the National Earthquake Hazards Reduction Program (NEHRP, 1997) site classification, which is used in AB2003. The generic rock and generic soil classes used in Y1997 were intended to be consistent with the Boore *et al.* (1993) site classes and hence can be translated to NEHRP classes. Because the C2004 model is an adjustment of the AB2003 model, the same NEHRP classes are used. The schemes used by Mc2006 and Z2006 include guidance regarding equivalent NEHRP site classes. LL2008 also uses generic rock and soil site classes, which are equivalent to NEHRP B and C (for rock) and NEHRP D and E (for soil). The G2005 and AR2010 models are developed for Mexican rock sites, which are compatible with NEHRP site class B. Due to the limited data NEHRP site class B in the calibration datasets (less than 10% of the total data), the two Mexican models were tested against the entire calibration datasets, irrespective of site conditions. Finally, the BC2010 model explicitly uses the average V_{S30} values, which can be directly translated into NEHRP site class definitions.

Except for Y1997 and LL2008, all of the selected models assume that the total variability of the model may be partitioned into inter- and intraevent variability components. The formulation of the Y1997 model partitions the total variability into intra- and interevent components; however, only the total variability is reported in the publication. The performance of these two models based on intra- and interevent residuals distributions is therefore not evaluated herein.

Visual Comparison of Selected Models

The scaling of the selected subduction models at rock sites over a range of spectral ordinates is compared in Figures 2 and 3, for interface and intraslab events respectively. Note that in these figures, the hypocentral distance (the distance metric used in the LL2008 model and BC2010 intraslab equation) was assumed to be equal to the rupture distance. Additionally, several of the models are extrapolated beyond their strict limits of applicability, but this is considered appropriate in the context of this study because such extrapolations are routinely made when GMPEs are applied in PSHA.

Figure 2 suggests a relatively low level of agreement amongst the predictions for interface earthquakes, particularly in terms of near-source behavior and attenuation with distance. In the context of subduction-zone earthquakes, observations that are relatively far away from the source can still be considered to be near-source observations due to the larger spatial extent of the rupture, compared to crustal events of similar magnitude (e.g., Strasser *et al.*, 2010). As seen in this figure, the AB2003 model exhibits strong magnitude saturation, with a nearly flat attenuation curve for M_w 8.5 interface events at short distances. Furthermore, the AB2003 interface equation shows a strong magnitude dependence of the attenuation for interface events, with attenuation rates decreasing with increasing magnitude; the remaining candidate models show a more rapid decay with distance, for the M_w 8.5 interface event.

Despite being derived from completely different datasets, the interface equations of Mc2006 and LL2008 tend to produce similar amplitudes to the Y1997 equation at the various spectral ordinates. In the case of the Mc2006 equation, this similarity may be due to the fact that the Y1997 model provided the functional form and coefficients needed to constrain the near-source behavior of the New Zealand model. Both the Y1997 and AB2003 interface models also predict similar amplitudes for the M_w 8.5 interface event, possibly due to the overlapping of their datasets from $M_w \geq 7.5$

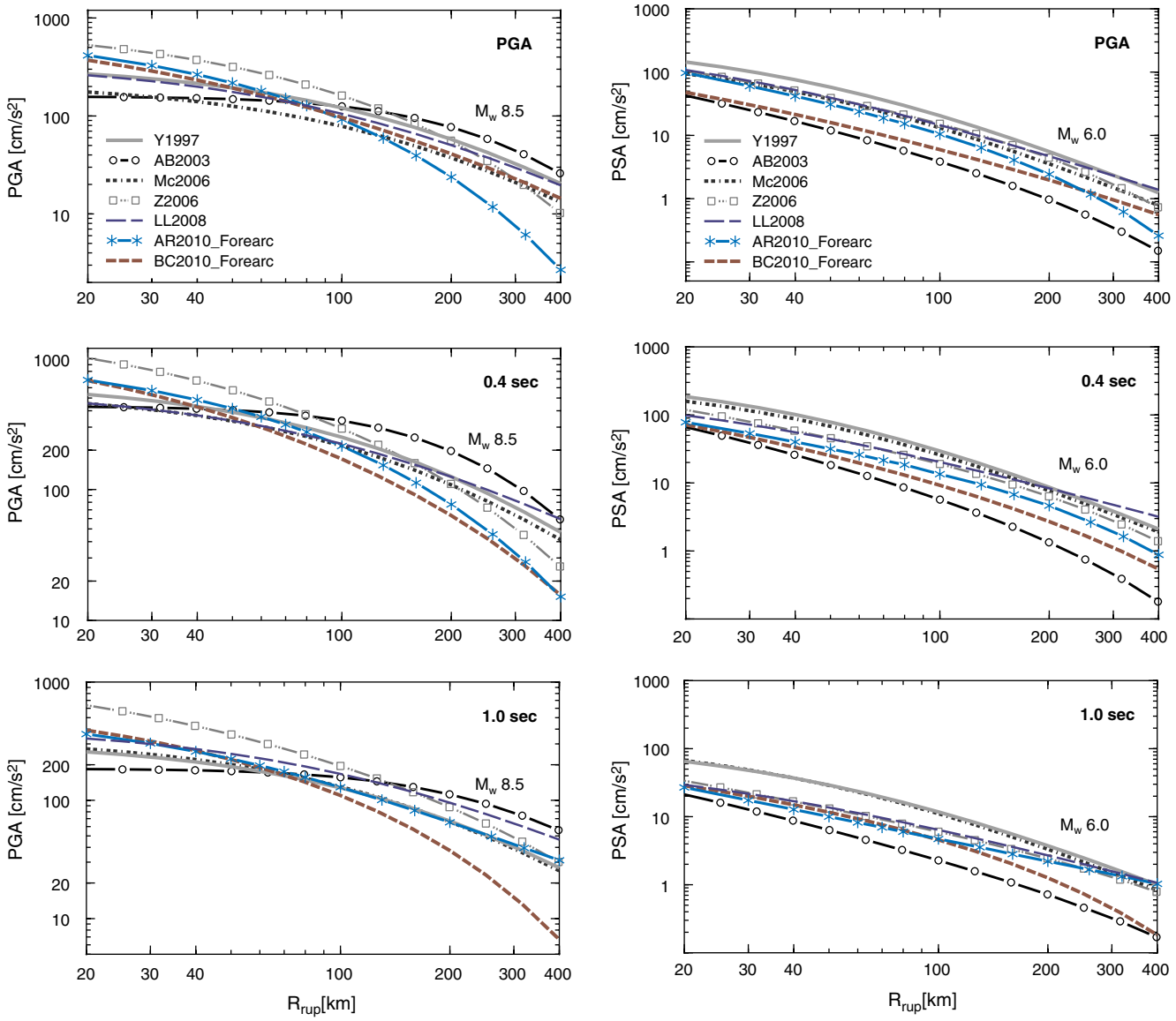

Figure 2. Comparison of the interface equations for magnitudes M_w 6.0 and 8.5, assuming a source depth of 30 km, over a range of spectral ordinates. In all cases, the plots shown correspond to rock conditions as defined by each model. The color version of this figure is available only in the electronic edition.

events. The Z2006 model predicts the largest amplitudes in the near-source region, although this effect may be caused by the fact that the near-source behavior of this model was constrained by shallow crustal data. For M_w 6.0 events, differences in decay rates among the models are not so pronounced. At this magnitude, both the AB2003 and BC2010 models tend to predict lower ground-motion amplitudes than do the other models.

In Figure 2, the BC2010 and AR2010 models reflect the attenuation behavior for forearc sites, based on global (but mainly Cascadia, Japan, and Taiwan) and Mexican data respectively. Several studies (e.g., Singh *et al.*, 2007; Kanno *et al.*, 2006; Macias *et al.*, 2008; Boore *et al.*, 2009; Arroyo *et al.*, 2010; BC Hydro 2010) have indicated a variation in the rate and characteristics of the attenuation between sites located in the forearc (i.e., between the subduction trench and volcanic front) and backarc regions (i.e., region landward of the volcanic front) and that this effect is more pronounced for intraslab motions. Although the amplitudes of the BC2010 and AR2010 models at distances of less than 100 km are comparable, their attenuation rates differ at longer distances.

Figure 3 presents the attenuation curves for intraslab events with magnitudes M_w 6.0 and 8.0 at rock sites over a range of response periods. Differences in terms of decay rate and near-source amplitudes among the selected intraslab equations are readily apparent from this figure. The Y1997 and Mc2006 intraslab equations exhibit a much slower rate of attenuation than do the other models and produce similar amplitudes. The LL2008 intraslab equation also shows a similar decay with distance, although it generally produces

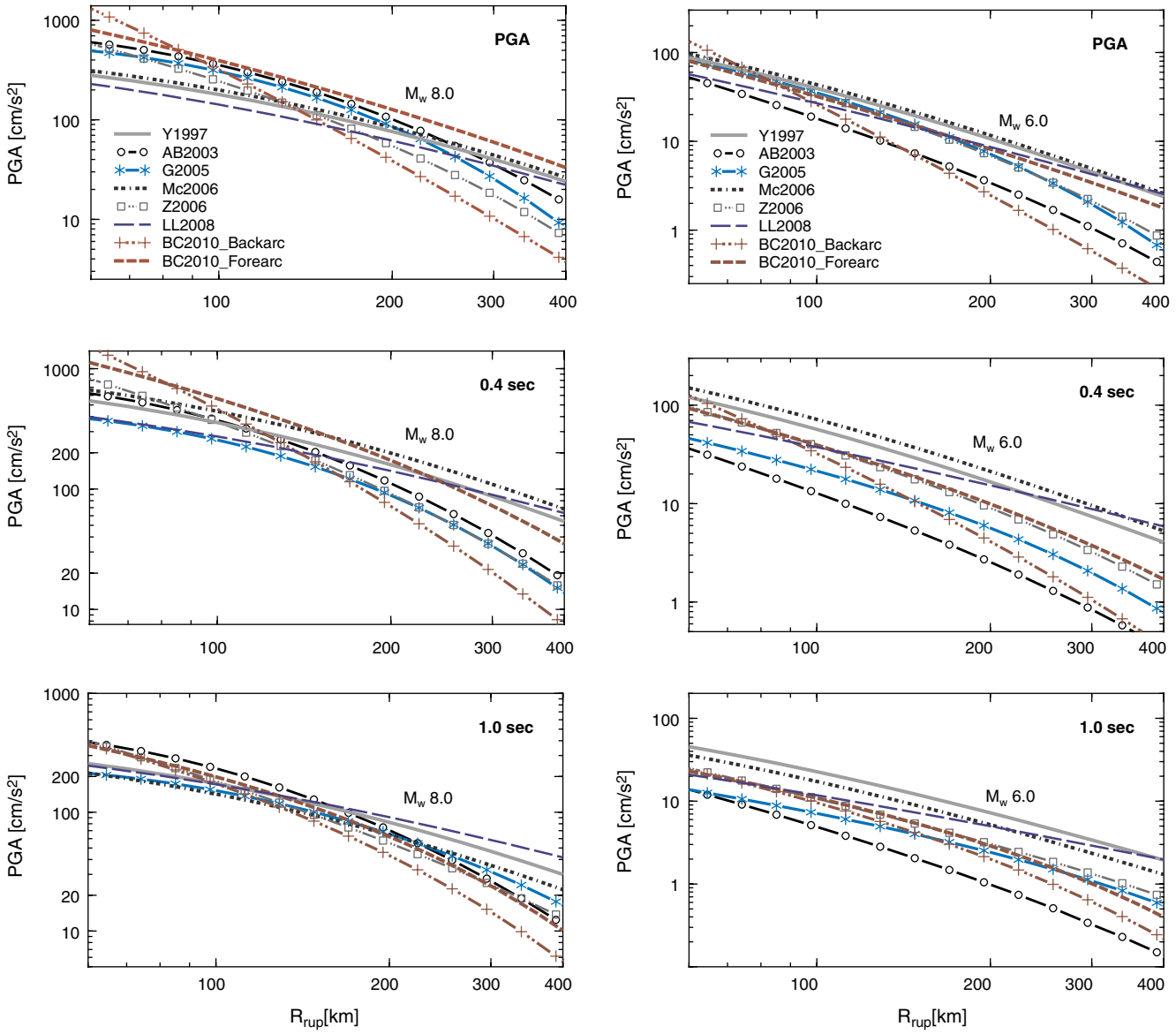

Figure 3. Comparison of the intraslab equations for magnitudes M_w 6.0 and 8.0, assuming a source depth of 75 km, over a range of spectral ordinates. In all cases, the plots shown correspond to rock conditions as defined by each model. The color version of this figure is available only in the electronic edition.

amplitudes that are lower than those of these two models. The early study of Y1997 included a limited number of intraslab records (53 out of 234 subduction records), so the behavior of this model is likely to be controlled by the interface data. For the M_w 8.0 intraslab event, both the intraslab equations of AB2003 and G2005 predict similar amplitudes and decay rate. At this magnitude, the Z2006 intraslab model also predicts amplitudes that are generally akin to those of the AB2003 and G2005 models. For events of magnitude M_w 6.0, the predictions of the AB2003 model are systematically lower than predictions from the other models; conversely, the amplitudes predicted by the Y1997 and Mc2006 models for the M_w 6.0 event tend to be larger than other predictions.

Figure 3 also indicates that important differences exist in the near-source amplitudes and decay rate between the BC2010 intraslab equations for forearc and backarc sites. The BC2010 backarc equation predicts larger amplitudes in the near-source region and a faster decay with distance than with the forearc model, especially for large magnitudes and for short periods. By comparison, the BC2010 forearc equation exhibits a much slower rate of attenuation, which is somewhat similar to that predicted by the Y1997 and Mc2006 equations for short periods. Figure 3 shows specific magnitude scenarios with a fixed depth of 75 km. All the selected models account for the effect of earthquake depth on the ground-motion amplitudes, which has a greater impact on intraslab ground motions. For a given magnitude and distance, high-frequency motions increase with increasing focal depth, but the depth effect is negligible for frequencies less than 1 Hz.

The differences in ground-motion amplitudes and attenuation behavior between interface and intraslab earthquakes are apparent from Figures 2 and 3. For events of similar magnitude, the equations for intraslab earthquakes tend to predict larger amplitudes in the near-source region than do interface equations. Furthermore, the AB2003 model shows a much stronger magnitude-dependence of the attenuation for interface events than for intraslab events. The models also exhibit differences between intraslab and interface events in terms of attenuation rates, with the ground motions associated with the former attenuating faster with distance; however, these differences are not so pronounced for the Y1997, Mc2006, and LL2008 models.

Performance of Selected Models

To evaluate the performance of the selected GMPEs in a quantitative manner, the predictions of the models are compared directly with the SAM and CAM datasets, using the method developed by Scherbaum *et al.* (2004). This method allows the ranking of a set of GMPEs according to their capability to predict recorded data, distinguishing between four categories (*A*, high predictive capability; *B*, intermediate capability; *C*, low capability; and *D*, unacceptable capability). These categories are defined by a number of statistical measures of the goodness-of-fit of a model to a sample dataset, including the mean, median, and standard deviation of the normalized total residuals (hereafter noted as MEAN [Z_T], MED [Z_T], and STD [Z_T], respectively) as well as the median value of the associated likelihood parameter distribution (MED [LH_T]). The likelihood parameter is a measure specifically developed for the purpose of evaluating ground-motion models and captures the effects of both the fit of the median and the shape of the underlying distribution of ground-motion residuals. We refer the reader to Scherbaum *et al.* (2004) for a detailed explanation of these goodness-of-fit measures. Additionally, the procedure described in Stafford *et al.* (2008), in which the total model variability is partitioned into interevent and intraevent components, is also implemented here in order to ensure that the results are not biased by correlations that may exist among residuals from the same event. The same notations are employed here as for the preceding statistical measures for the categories, but the subscripts are changed to reflect the component of variability considered: Z_A and Z_E refer to normalized intra- and interevent residuals, respectively, and LH_A and LH_E to the associated likelihood functions.

Interface Models

The equations for interface events of the Y1997, AB2003, Mc2006, Z2006, LL2008, AR2010, and BC2010 models have been tested with the separate SAM and CAM interface datasets. For the AB2003 model, the application of regional correction factors for South and Central America, as developed by Atkinson and Boore (2003), was investigated, but because the application of these factors only had a marginal impact on the performance of the model, the results are not presented. Instead, the effect of magnitude scaling is investigated for the CAM interface dataset, by assessing separately the performance of the model against data from events with $M_w < 6.0$ (AB2003_$M_w < 6.0$) and those from events with $M_w \geq 6.0$ (AB2003_$M_w \geq 6.0$) and comparing the results to those obtained using the full CAM interface dataset (AB2003_all_data). The equations of BC2010 and AR2010 for forearc sites are used for the SAM data, all of which were recorded at forearc locations. For the CAM data, 90% of recordings were obtained at such sites. Therefore, because the AR2010 interface model is only applicable to forearc sites, the 10% of CAM data from backarc sites were excluded when testing this model. For the BC2010 model, the full CAM dataset was used with appropriate settings on the forearc/backarc term.

The rankings determined for each selected equation, for the full range of spectral ordinates considered, are listed in Table 3. The results obtained in terms of the goodness-of-fit measures MEAN [Z_X], MED [Z_X], STD [Z_X], and MED [LH_X], where the subscript X reflects the component of variability considered (T, total; A, intraevent; E, interevent) are listed in extended versions of this table available as Ⓔ Tables S1 (SAM data) and S2 (CAM data) of the electronic supplement to this paper. Figure 4 shows the distributions of the normalized total residuals (Z_T) and associated likelihood values (LH_T) obtained from the SAM interface dataset and the selected equations for PGA and PSA at 1.0 s. Similarly, Figure 5 shows Z_T and LH_T distributions for the CAM interface dataset. Based on these distributions, a model is considered to perform well if the distribution of the residual values agrees well with the standard normal distribution, indicating that the model is unbiased and that the standard deviation of the model captures the variability in the recorded data. Evenly distributed likelihood values also indicate that the model is unbiased and that the shape of the residual distribution is consistent with the variability specified in the model. The results obtained using the interevent and intraevent components of variability are shown plotted against response period in Figures 6 and 7 for the SAM and CAM datasets, respectively.

Overall, these results show a variable performance of the selected models across response periods, as well as differences in the quality of fit between the CAM and SAM datasets. Generally, the summary statistics of the normalized intraevent model residuals (Z_A) and their associated likelihood values (LH_A) indicate a better level of agreement between predictions and recorded data compared to total normalized residuals, suggesting that the mismatch between predictions and observations stems from event-specific processes related to the source and possibly the path, rather than from site-specific factors. This is also indicated by the larger absolute values of the normalized interevent model residuals (Z_E), which appear to be associated with more pronounced differences between the various models than their intraevent equivalents. It is also interesting to note that interevent residuals for the SAM dataset take positive values at periods less than 1 s for all models, which could suggest a region-specific

Table 3
Ranking of Selected Models for Prediction of Interface Motions in South and Central America*

Interface Models†	PGA	(P)SA$_{5\%}$ 0.04 s	(P)SA$_{5\%}$ 0.10 s	(P)SA$_{5\%}$ 0.20 s	(P)SA$_{5\%}$ 0.40 s	(P)SA$_{5\%}$ 1.00 s	(P)SA$_{5\%}$ 2.00 s	(P)SA$_{5\%}$ 3.00 s
Peru–Chile								
Y1997_soil	B/-/-	-/-/-	B/-/-	A/-/-	B/-/-	B/-/-	B/-/-	B/-/-
Y1997_rock	A/-/-	-/-/-	B/-/-	B/-/-	B/-/-	B/-/-	A/-/-	A/-/-
AB2003	B/B/C	C/B/C	B/B/C	B/B/D	B/B/C	B/A/B	A/A/A	A/A/A
Mc2006	D/C/D	-/-/-	D/B/D	B/A/B	C/C/B	C/B/A	D/B/B	B/B/B
Z2006	B/A/B	A/A/B	A/A/B	B/A/B	B/A/B	B/A/A	C/B/B	D/B/C
LL2008	D/-/-	D/-/-	D/-/-	D/-/-	C/-/-	B/-/-	B/-/-	C/-/-
AR2010	C/B/C	B/B/C	B/B/C	C/B/D	D/C/D	C/C/C	B/B/B	B/B/C
BC2010	C/B/C	B/B/C	B/A/C	B/A/C	C/B/C	A/A/B	B/A/A	C/B/A
Central America								
Y1997	C/-/-	-/-/-	B/-/-	B/-/-	B/-/-	B/-/-	B/-/-	A/-/-
AB2003_all data	D/C/D	D/B/D	D/C/D	D/C/D	D/C/D	D/B/D	B/A/C	B/A/B
AB2003_M_w <6.0	D/D/-	D/D/-	D/D/-	D/D/-	D/D/-	D/B/-	C/B/-	C/B/-
AB2003_M_w ≥6.0	B/A/B	B/A/B	B/A/B	B/A/B	C/B/B	B/A/B	B/A/A	A/A/A
Mc2006	A/A/B	-/-/-	B/A/A	B/B/B	B/B/B	B/A/A	C/B/C	B/B/B
Z2006	B/A/B	B/A/B	A/A/B	B/A/B	B/A/A	A/A/A	B/A/B	B/A/B
LL2008	B/-/-	B/-/-	A/-/-	A/-/-	A/-/-	A/-/-	B/-/-	B/-/-
AR2010	C/A/C	B/A/C	C/A/C	C/A/D	D/A/D	C/A/D	C/A/C	C/A/C
BC2010	C/A/C	B/A/C	C/A/B	B/A/C	C/B/C	B/A/B	A/A/A	A/A/A

*In each case, a triplet of rankings $R_T/R_A/R_E$ is provided, in which the subscript identifies the type of normalized residuals and likelihoods used to determine the rankings. (For rankings: *T*, total; *A*, intraevent; *E*, interevent.)

†Interface models: Y1997, Youngs *et al.* (1997); AB2003, Atkinson and Boore (2003); Mc2006, McVerry *et al.* (2006); Z2006, Zhao *et al.* (2006); LL2008, Lin and Lee (2008); AR2010, Arroyo *et al.* (2010); BC2010, BC Hydro (2010).

feature of the interface-type events along the Peru–Chile subduction zone.

Among the selected models, the Japanese model of Z2006 appears to match the observed data best: for both datasets and regardless of which type of residual is considered, this model is ranked as either A or B, except for the SAM results based on Z_T for 2 and 3 s, where it is biased toward negative residual values and hence is ranked as class C and D. For the CAM dataset, the only characteristic that prevents this model from being ranked as class A for all periods is its small bias toward overprediction, as indicated by the central tendency measures, which generally take negative values. Overall, this model is found to be generally unbiased (the central tendency measures are close to 0) with respect to the recorded data and successful in capturing their variability (STD$[Z_X] \approx 1$). It is noteworthy that the standard deviations of this model are up to 0.1 $\log_{10}$ units larger than those of other candidate models, such as AB2003 and Mc2006, which are associated with less consistent results across datasets and response periods.

While showing some inconsistency across response periods, the Y1997 model has a similar predictive capability for both datasets and is generally ranked as B. Note that for the SAM dataset, data from NEHRP C sites have been compared to the Y1997 models for generic rock (Y1997_rock) and soil (Y1997_soil) to assess whether the classification of these sites could influence the quality of the predictions. The resulting Z_T distributions for the SAM dataset following the soil or rock assumption for NEHRP C data (Fig. 4) indicate that, in both cases, the Y1997 model captures the central tendency values and the standard deviation well for all periods. Conversely, for the CAM interface subset, the Y1997 model consistently overpredicts the observed values, and the standard deviation of the model is considerably larger than the variability of the observed data (STD$[Z_T] < 1$). The Y1997 model has a magnitude-dependent standard deviation that becomes unusually large for small-to-moderate magnitude events, varying from 0.41 $\log_{10}$ units at M_w 5.0 to 0.37 $\log_{10}$ units at M_w 6.0, and hence analyses based on normalized model residuals may not provide a strong indication regarding the performance of this model. This does not necessarily imply that the overall variability of this model has been overestimated—only that in using a heteroscedastic model the equation has excessively high sigma values for smaller events. For the CAM dataset, this model is generally ranked as B for most periods, similar to the performance of the Y1997_soil model for the SAM dataset.

As seen in Figure 4, the AB2003 interface model for PGA is predominantly unbiased when compared to the SAM dataset, but the standard deviation of the data is larger than the standard deviation of the model. This is also observed from the distribution of LH_T values, which shows a greater frequency of low LH_T values, although the performance of the model improves at longer periods. The summary statistics based on the total residuals show that this model is associated with the highest and intermediate predictive capabilities (ranks A and B), except for an instance at 0.04 s, at which it is ranked as C. On the basis of the intraevent residuals (Z_A) of the SAM dataset, the AB2003 model is ranked as class B for periods less than 1 s, mainly because of the large standard

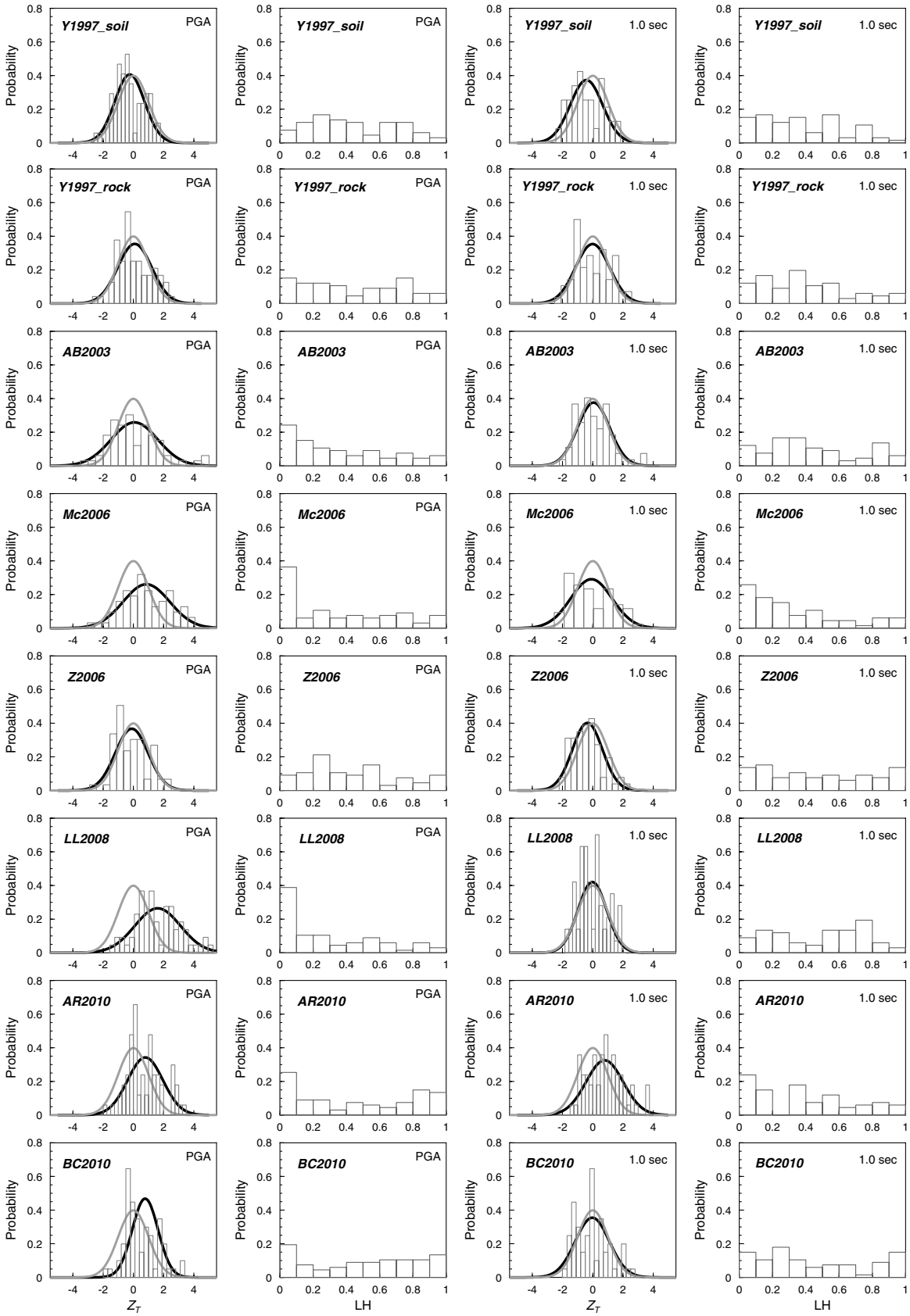

Figure 4. Distributions of the normalized total model residuals (Z_T) and associated likelihood values (LH_T) for the selected equations at PGA and 1 s, tested against the SAM interface dataset. The plots of the normalized model residuals also include the standard normal distribution (*gray solid line*) and the normal distribution fitted to the residuals (*black solid line*).

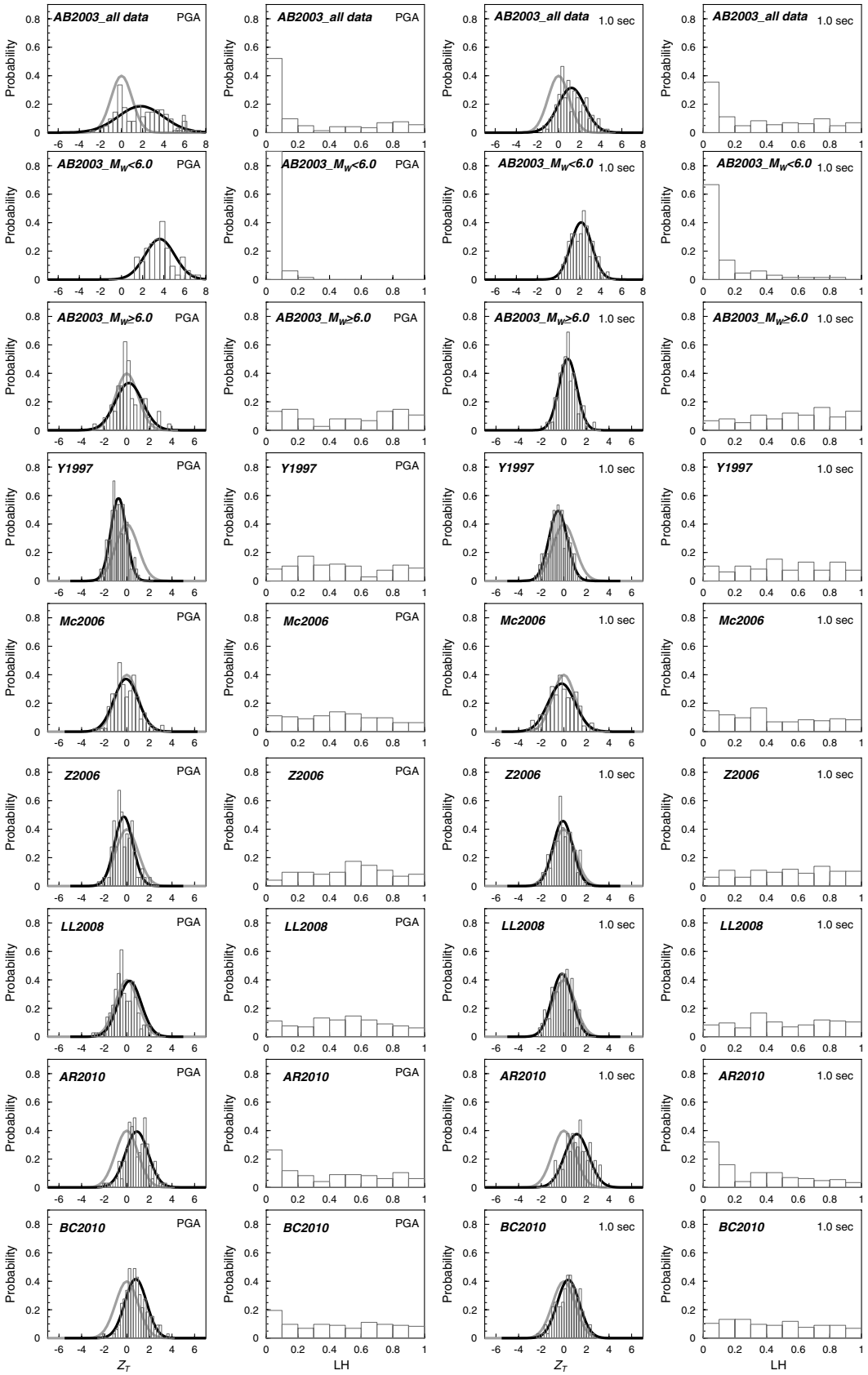

Figure 5. Distributions of the normalized total model residuals (Z_T) and associated likelihood values (LH_T) for the selected equations at PGA and 1 s, tested against the CAM interface dataset. The plots of the normalized model residuals also include the standard normal distribution (gray solid line) and the normal distribution fitted to the residuals (black solid line).

deviation of the intraevent residuals (STD[Z_A] > 1.25), indicating that the spatial variability of the ground motions in the subduction zone under study is greater than the variability of the model, even though about half of the data used for this comparison was used for the development of the AB2003 interface model.

The AB2003 model performs very poorly, however, in terms of predicting the CAM data, except at long periods, and is mostly ranked as D on the basis of the Z_T distribution. An examination of the total residuals for the AB2003 model with respect to various explanatory variables indicated a trend of increasing Z_T values with decreasing magnitude,

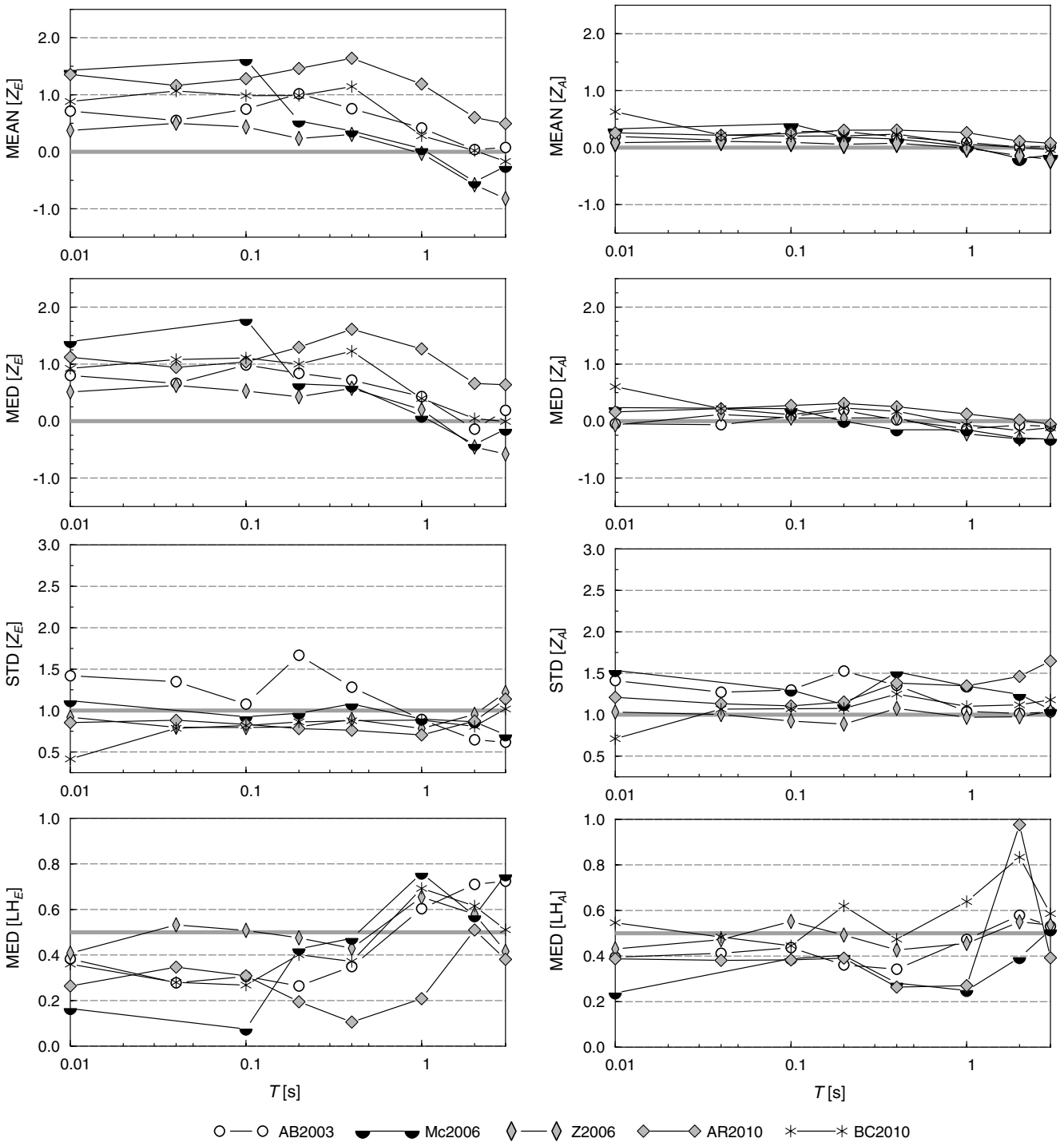

Figure 6. Goodness-of-fit measures associated with the normalized interevent (Z_E) and intraevent (Z_A) model residuals for selected interface equations, tested against the SAM dataset. The thick gray lines show the target values: MEAN [Z_X] and MED [Z_X] = 0; STD [Z_X] = 1.0; and MED [LH_X] = 0.5. Note that the Y1997, C2004, and LL2008 models are not included (see text for details).

taking values of 4 and larger for magnitudes less than M_w 6.0 and for periods less than 1 s. Therefore, the performance of this model is further analyzed using subsets of the CAM data from $M_w < 6.0$ (AB2003_$M_w < 6.0$) and $M_w \geq 6.0$ (AB2003_$M_w \geq 6.0$) events in addition to the entire CAM interface database (AB2003_all data). The Z_T values for PGA for AB2003_all data exhibit a bimodal distribution with two central values, one at about 0 and another at 4 (Fig. 5). A normal distribution fitted to the normalized total residuals would therefore have a large standard deviation (STD[Z_A] > 2). The median values of the likelihood parameter are close to zero (MED[LH_T] < 0.10), reflecting

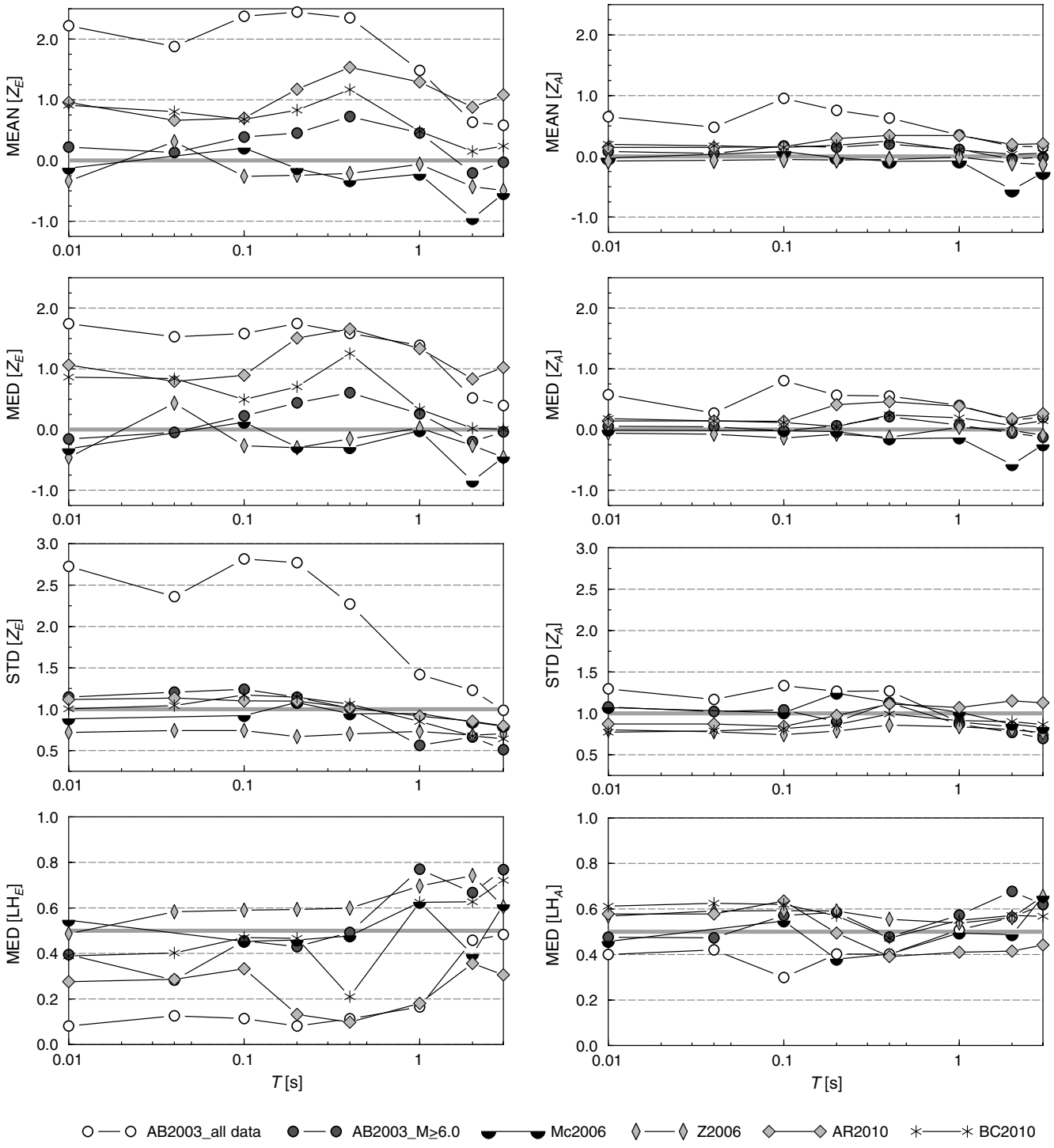

Figure 7. Goodness-of-fit measures associated with the normalized interevent (Z_E) and intraevent (Z_A) model residuals for selected interface equations, tested against the CAM dataset. The thick gray lines show the target values: MEAN[Z_X] and MED[Z_X] = 0; STD[Z_X] = 1.0; MED[LH_X] = 0.5. Note that the Y1997, C2004 and LL2008 models are not included (see text for details).

the poor fit to the data. Although the bimodal pattern does not persist when the model is tested against small magnitude data (AB2003_M_w <6.0), the model continues to underestimate the recorded values. However, the summary statistics for the $M_w \geq 6.0$ subset of data show a reasonable match to the data, both in terms of central tendency measures and in terms of variability. This results in a category B ranking at most spectral ordinates, except for 0.4 s, at which the model is ranked as class C because of its bias.

The large positive residuals observed for the AB2003 model for M_w <6.0 data could reflect the inadequacy of the magnitude scaling term of this equation to model data in this magnitude range, which lies outside the intended magnitude range of applicability of the model, although a limited number of records from M_w <6.0 events were included in the database for regression (less than about 8%). Atkinson and Boore (2003) reported large positive residuals for events of magnitudes M_w <6.5 in their database, which they attributed to the linear form used for the magnitude term. It should also be noted that the AB2003 model has the lowest total aleatory variability amongst the candidate models and therefore, for the same difference between predicted and observed values, results in larger normalized residual values than other models.

Examination of the summary statistics with derivations based on Z_A and Z_E confirms that the poor performance of this model for the CAM dataset is related essentially to event-specific factors resulting in underprediction at smaller magnitudes. In terms of Z_A, the AB2003 model is ranked as class A and B at periods longer than 0.4 s and as class B and C at shorter periods. However, when considering the interevent model residuals, the AB2003 model (AB2003_all data) is ranked as class D at periods up to 1 s and ranked C and B at 2 and 3 s. The interevent residuals are strongly biased (MEAN[Z_E] ~ 2.5) and the associated standard deviation (STD[Z_E]) takes large values (>2.0) at periods less than 1 s. The median values of the likelihood parameter are very low (MED[LH_T] < 0.10) indicating a low predictive capability. Note that the standard deviation of the normalized interevent residuals for this model generally takes values greater than 1.0, denoting that variability of the data related to event-specific processes is larger than that considered by this model. The performance of the model improves when the $M_w \geq$ 6.0 subset of CAM data is considered, with Z_E-based rankings of A or B for all spectral periods considered.

The performance of the Mc2006 model shows a marked dependency on response period, as well as on the dataset considered. For the SAM data, the Mc2006 model for PGA is strongly biased and does not adequately capture the data standard deviation, although the performance of the model improves at 1 s. This model shows an unacceptable capability (rank D) to predict the data at very short periods (≤0.1 s) and at 2 s. At the remaining spectral ordinates, the model is ranked as class B and C. The results based on the normalized interevent (Z_E) model residuals indicate that the quality of the predictions of this model varies substantially across the range of periods considered. For instance, MEAN[Z_E] and MED[Z_E] take large positive values at short periods (≤0.2 s) and the associated MED[LH_E] values are very low, indicating the low predictive capability of the model in this period range. At periods beyond 0.2 s, however, the model performs reasonably well. For the CAM dataset, the Mc2006 model is also ranked as class B or A at all periods except for 2.0 s, where the model is ranked as class C because of its large bias in terms of Z_E.

Similarly, the performance of the LL2008 model shows a marked dependency on the dataset and response period considered. For the SAM data and periods of less than 0.4 s, this model is strongly biased and fails to capture the standard deviation of the data; it therefore is ranked as class C and D. For longer periods, the performance of this model somewhat improves, and it is ranked as class B and C. Examination of total normalized residuals with respect to distance indicates a trend of increasing Z_T values with decreasing distance, taking values as large as 5. The mismatch between the SAM data and predictions could therefore be due to the use of the hypocentral distance as distance metric, which poorly discriminates between sites located directly above the rupture plane and those located a significant distance away. This is particularly relevant for the SAM interface dataset, which mostly comes from large interface events associated with a large spatial extent of the rupture plane. We note, however, that the performance of this model improves when tested against the CAM dataset, for which it is generally ranked as class A and B because of its small bias with MEAN[Z_T] and MED[Z_T] taking negative values. As seen in Figure 1, most of the CAM interface data come from small-to-moderate size events, which are associated with smaller rupture dimensions, and hence the use of the hypocentral distance may be a valid approximation.

The BC2010 and AR2010 equations for forearc sites also show a strong dependency on response period in their predictive capability. For the SAM data, the BC2010 model tends to underpredict the data at PGA and periods less than 1 s, and it is hence ranked as class B and C based on the Z_T distribution. The AR2010 model for forearc sites also consistently underpredicts the data at most spectral ordinates and has therefore been ranked as class B and C, except for an instance at 0.4 s, where it is ranked as class D. Similar patterns are observed for the CAM interface data, for which the BC2010 model tends to underpredict the interface data at periods less than 1 s. Examination of the normalized residuals (Z_T) of this model with respect to magnitude also shows a trend, with Z_T values of 3 and larger for magnitudes less than M_w 6.0 and for periods less than 1 s. The BC2010 model is therefore ranked as class C and B for periods less than 1 s and class A at longer spectral ordinates. Examination of the Z_E and Z_A distributions reveals that, as for the AB2003 model, this behavior appears to be controlled by event-specific factors because this model is generally ranked as class A on the basis of the Z_A values.

Intraslab Models

The intraslab equations of Y1997, AB2003, G2005, Mc2006, Z2006, LL2008, and BC2010 have been tested against the SAM and CAM intraslab datasets. For the CAM dataset, the C2004 equation, derived through modification of the AB2003 intraslab equation using locally recorded data, was also included. Because nearly 85% of the SAM intraslab dataset were recorded at NEHRP C sites, it was necessary to assess whether the classification of NEHRP C sites as generic rock or generic soil could influence the quality of the predictions for the Y1997 model. For the SAM dataset, NEHRP site C data have therefore been compared to the Y1997 models for generic rock (Y1997_rock) and for generic soil (Y1997_soil).

The distributions of the normalized total model residuals (Z_T) and associated likelihood values (LH_T) calculated from the SAM intraslab dataset are shown in Figure 8, for PGA and spectral (or pseudospectral) acceleration at 1 s. The rankings assigned to each model for the range of response periods considered are listed in Table 4; a full listing of the summary results is available in Ⓔ Table S3 of the electronic supplement to this paper. Figure 9, Table 4, and Ⓔ Table S4 of the electronic supplement present the equivalent information for the CAM dataset. Finally, Figures 10 and 11 present the summary statistics based on Z_E and Z_A for each dataset and for those models for which estimates of the intra- and interevent components of variability are provided.

The results suggest that the performance of the selected models varies significantly across spectral periods and again appears to depend on the dataset considered, with BC2010 being the only model that performs consistently well. This model is generally unbiased and is therefore associated with the highest and intermediate predictive capabilities (ranks A and B). The Z2006 model for Japan also shows a good performance overall, particularly for the CAM dataset, where it is consistently ranked A or B. While it largely underpredicts the short-period data ($\leq$0.1 s) for the SAM dataset, leading to a class C ranking, it shows an improved predictive capability at longer periods. It is noteworthy that the observed variability of the SAM intraslab data has been found to be lower than the standard deviations of the various models ($STD[Z_T] < 1.0$ and $STD[Z_E] < 1.0$), possibly due to the limited number of earthquakes (five) represented in the dataset. Conversely, for the CAM dataset, the standard deviations of the various models tend to be smaller than the sample standard deviation, particularly for periods longer than 0.2 s.

For the SAM dataset, the assessment across the spectral periods shows that the AB2003 intraslab model reasonably predicts the median ground motions at PGA, 1 and 2 s, but largely underpredicts the data at periods between 0.1 and 0.4 s (i.e., $MEAN[Z_T]$ and $MED[Z_T]$ values >0.75). The G2005 model shows a similar pattern of underprediction at these periods. Both equations are associated with the lowest prediction capabilities (ranks C and D) at periods between 0.1 and 0.4 s. For the remaining response periods, the AB2003 and G2005 models are ranked as class A and B. The results for the Y1997 model suggest that the performance of this model depends upon the manner in which the motions at NEHRP class C sites are modeled, with the Y1997_soil case better fitting the data at PGA, 0.2 and 0.4 s (rank A and B) and Y1997_rock case better matching the data at longer periods. The Mc2006 model for New Zealand performs well in predicting the median values and hence is ranked as class B, except for one instance at 0.1 s, where a rank C has been assigned because of its large bias. On the basis of the intraevent residuals (Z_A), all of the selected models generally perform better, although the central tendency measures ($MEAN[Z_A]$ and $MED[Z_A]$) for the AB2003 and G2005 models continue to indicate some degree of underprediction at periods between 0.1 and 0.4 s. The mean interevent residuals for the AB2003 and G2005 models follow a similar pattern across the spectral periods, with $MEAN[Z_E]$ and $MED[Z_E]$ taking values as high as 1.0 at 0.2 and 0.4 s. The opposite is observed for the Z2006 and Mc2006 models, which are associated with large $MEAN[Z_E]$ and $MED[Z_E]$ values in the short-period range ($\leq$0.1 s).

A comparison of the summary statistics based on Z_T and those based on Z_E suggests that the mismatch between observed data and predictions of the various models is most likely to be controlled by event-specific factors such as differences in the scaling of ground-motion amplitudes with magnitude. Overall, the different goodness-of-fit measures analyzed indicate that the BC2010, Mc2006, and Z2006 equations satisfactorily predict the recorded intraslab data used for this comparison across the range of periods considered. The fact that the G2005 model, which only considers rock sites, is ranked as class B on the basis of Z_A values suggests that the quality of the predictions of this model is not strongly dependent upon the modeling of the site conditions but instead depends upon the modeling of event-specific source, and possibly path, characteristics.

For the CAM dataset, the BC2010 and Z2006 models adequately capture both the central tendency and the variability of the observed data. The AB2003 global model largely underpredicts the observed motions for periods $T \geq 0.2$ s, as given by the central tendency measures ($MEAN[Z_T]$ and $MED[Z_T]$), which take generally positive values. The G2005 equation for rock sites adequately predicts median observed values at short periods (<0.2 s); however, this model largely underpredicts the data at longer periods, which might be due to the response of soil sites, which represent a significant part of the database, not being specifically modeled by this equation. Both the Mc2006 and C2004 equations strongly overpredict the CAM intraslab data ($MEAN[Z_T] > 1.0$). The distributions of LH values for these two models show a greater number of low LH values, indicating their low predictive capability. The Y1997 equation slightly tends to overpredict the data. The results in Table 4 indicate that BC2010 and Z2006 are the only models ranked as class A and B across the selected spectral periods. The Y1997 model also produces satisfactory predictions and is ranked as class B and C. The global model of AB2003 is ranked as class D for periods

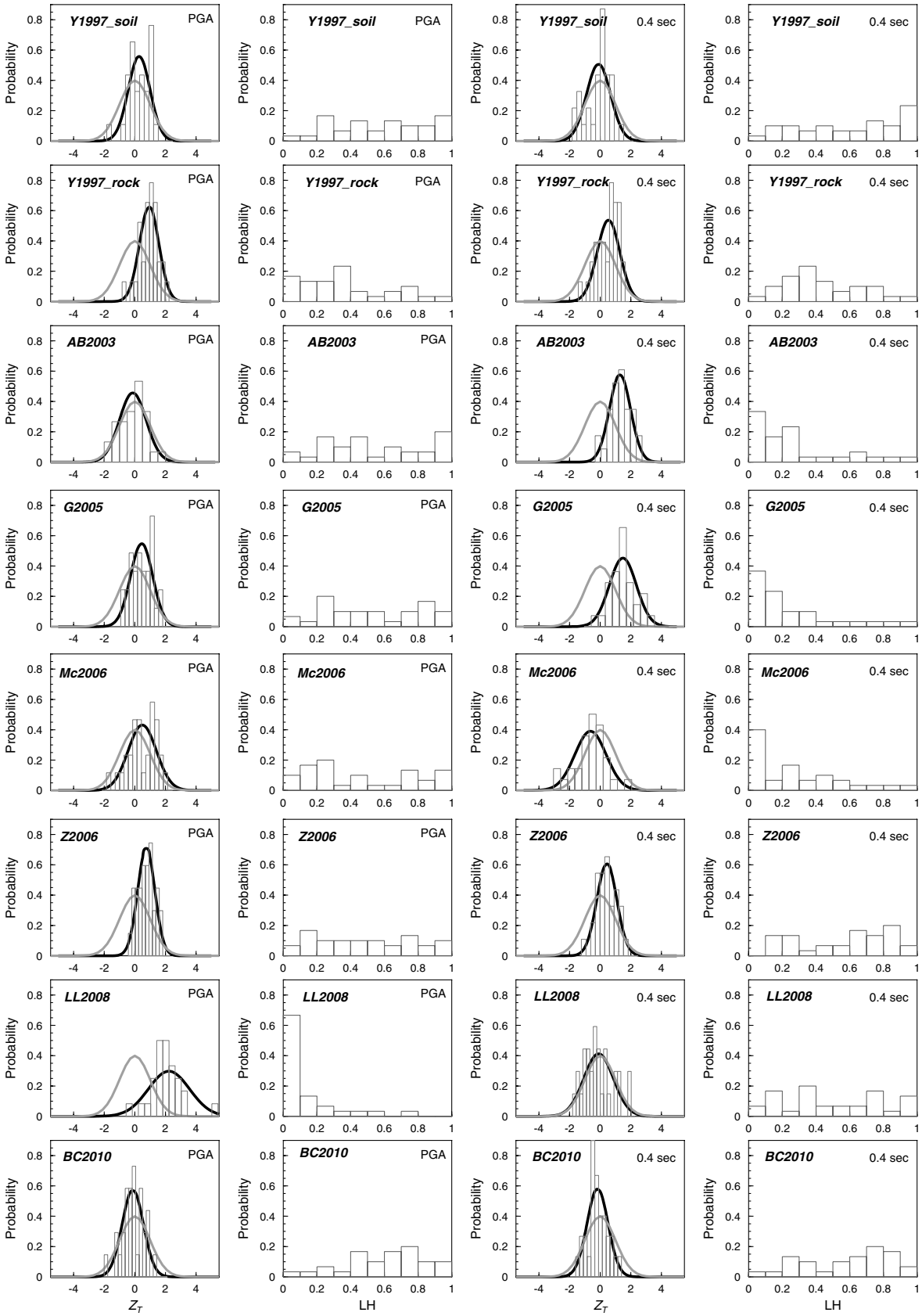

Figure 8. Distributions of the normalized total model residuals (Z_T) and associated likelihood values (LH_T) for the selected equations at PGA and 1 s, tested against the SAM intraslab dataset. The plots of the normalized model residuals also include the standard normal distribution (gray solid line) and the normal distribution fitted to the residuals (black solid line).

longer than 0.2 s because of its strong bias. At shorter periods the AB2003 model is ranked as class B. Similarly, the G2005 model is ranked as class A and B at periods less than 0.2 s, but the model has an unacceptable predictive capability at longer periods (class D). Finally, the C2004 model is ranked as class D and C for the two spectral periods for which coefficients are available.

The results for the Z_A and Z_E distributions for the AB2003, G2005, Z2006, and Mc2006 models show that these models generally improve their ranking for the CAM dataset on the basis of the Z_A distributions, although the AB2003 and G2005 models show a slight tendency to underpredict the spectral accelerations above 0.1 s. A similar pattern is observed in the distributions of the normalized interevent residuals (Z_E) for the AB2003 and G2005 models, which are also biased towards positive values (MEAN$[Z_E] > 1.0$), indicating significant underprediction. These results indicate that the AB2003 and G2005 models are, in general, associated with class A and B rankings on the basis of their intraevent residuals, although these models have a low predictive capability (class C) at 0.4 s. The analyses suggest that the distributions of intraevent residuals for the Mc2006 model only show a slight tendency to overpredict the data, but the Z_E values are significantly biased across most of the periods used for this comparison. Both the intra- and interevent normalized residuals distributions for the Z2006 model show an adequate fit to the data in terms of both median values and variance. On the basis of the interevent normalized residuals, three of these models (AB2003, G2005, Mc2006) perform well at short periods ($\leq$0.2 s) and are ranked as class B, but at longer periods they are ranked as class D because of their large bias (MEAN$[Z_A]$ and MED$[Z_A] > 1.0$) and standard deviation, which is smaller than that of the observed data that is also reflected in the low LH values (< 0.2). The Mc2006 model shows a very poor fit at most of the selected periods when considering the interevent residuals and is ranked as class C and D, except for an instance at 1.0 s, at which the model is ranked as class B. The BC2010 and Z2006 models remain the only ones to be ranked as class A and B on the basis of the intraevent and interevent residuals, respectively.

When tested against the SAM intraslab dataset, the LL2008 model again shows a poor performance at periods of less than 0.4 sec and is ranked as class D on the basis of the total model residuals. The model is largely biased (MEAN$[Z_T]$ and MED$[Z_T] > 2.0$) and fails to capture the standard deviation of the observed SAM data. We did not observe a clear trend in the residuals with distance or magnitude and believe these differences are possibly due to the fact that this regional model generally tends to predict lower amplitudes for large intraslab events (see Fig. 3). For the CAM dataset, the LL2008 model performs consistently well across the response periods examined and is generally ranked as class B because of its small bias.

Discussion

The results presented herein indicate a large variation in the performance of the models depending on response period, regional dataset (SAM or CAM), and type of event (interface or intraslab) considered. It should be noted, however,

Table 4
Ranking of Selected Models for Prediction of Intraslab Motions in South and Central America*

Intraslab Models†	PGA	(P)SA$_{5\%}$ 0.04 s	(P)SA$_{5\%}$ 0.10 s	(P)SA$_{5\%}$ 0.20 s‡	(P)SA$_{5\%}$ 0.40 s	(P)SA$_{5\%}$ 1.00 s	(P)SA$_{5\%}$ 2.00 s	(P)SA$_{5\%}$ 3.00 s
Peru–Chile								
Y1997_soil	B/-/-	-/-/-	C/-/-	B/-/-	A/-/-	D/-/-	C/-/-	B/-/-
Y1997_rock	C/-/-	-/-/-	D/-/-	C/-/-	C/-/-	A/-/-	A/-/-	A/-/-
AB2003	A/A/B	B/A/A	C/B/C	D/B/D	D/B/C	A/A/A	B/B/A	D/B/C
G2005	B/B/B	B/B/B	C/B/C	C/B/D	D/B/D	B/A/B	B/A/A	B/A/B
Mc2006	B/B/C	-/-/-	C/B/C	B/A/A	B/A/B	A/A/A	B/A/B	B/B/B
Z2006	C/A/C	C/B/D	C/B/C	B/A/B	B/A/B	A/A/A	B/B/B	B/A/B
LL2008	D/-/-	D/-/-	D/-/-	D/-/-	D/-/-	A/-/-	A/-/-	A/-/-
BC2010	A/A/B	A/A/B	B/A/C	A/B/B	B/A/A	B/B/A	B/A/B	B/A/B
Central America								
Y1997	B/-/-	-/-/-	B/-/-	B/-/-	B/-/-	C/-/-	B/-/-	A/-/-
AB2003	B/A/B	B/A/B	C/B/B	D/B/D	D/C/D	D/B/D	C/B/D	D/B/D
C2004	D/-/-	-/-/-	-/-/-	C/-/-	-/-/-	C/-/-	-/-/-	-/-/-
G2005	B/A/B	A/A/A	A/A/A	C/B/D	D/C/D	D/C/D	D/B/D	D/B/D
Mc2006	D/B/D	-/-/-	C/A/C	D/B/D	D/B/D	C/B/B	C/B/D	B/A/C
Z2006	B/A/B	B/A/B	A/A/A	A/A/B	A/A/B	A/A/A	A/A/B	B/A/B
LL2008	B/-/-	B/-/-	A/-/-	B/-/-	B/-/-	B/-/-	B/-/-	B/-/-
BC2010	B/A/B	B/A/B	A/A/B	A/A/A	A/A/B	B/A/B	B/A/B	B/A/B

*In each case, a triplet of rankings $R_T/R_A/R_E$ is provided, in which the subscript identifies the type of normalized residuals and likelihoods used to determine the rankings. (For rankings: *T*, total; *A*, intraevent; *E*, interevent.)

†Interface models: Y1997, Youngs *et al.* (1997); AB2003, Atkinson and Boore (2003); G2005, García *et al.* (2005); Mc2006, McVerry *et al.* (2006); Z2006, Zhao *et al.* (2006); LL2008, Lin and Lee (2008); BC2010, BC Hydro (2010); C2004, Cepeda *et al.* (2004).

‡Because the C2004 model does not provide coefficients at this period, the analysis for 0.3 s is used as proxy.

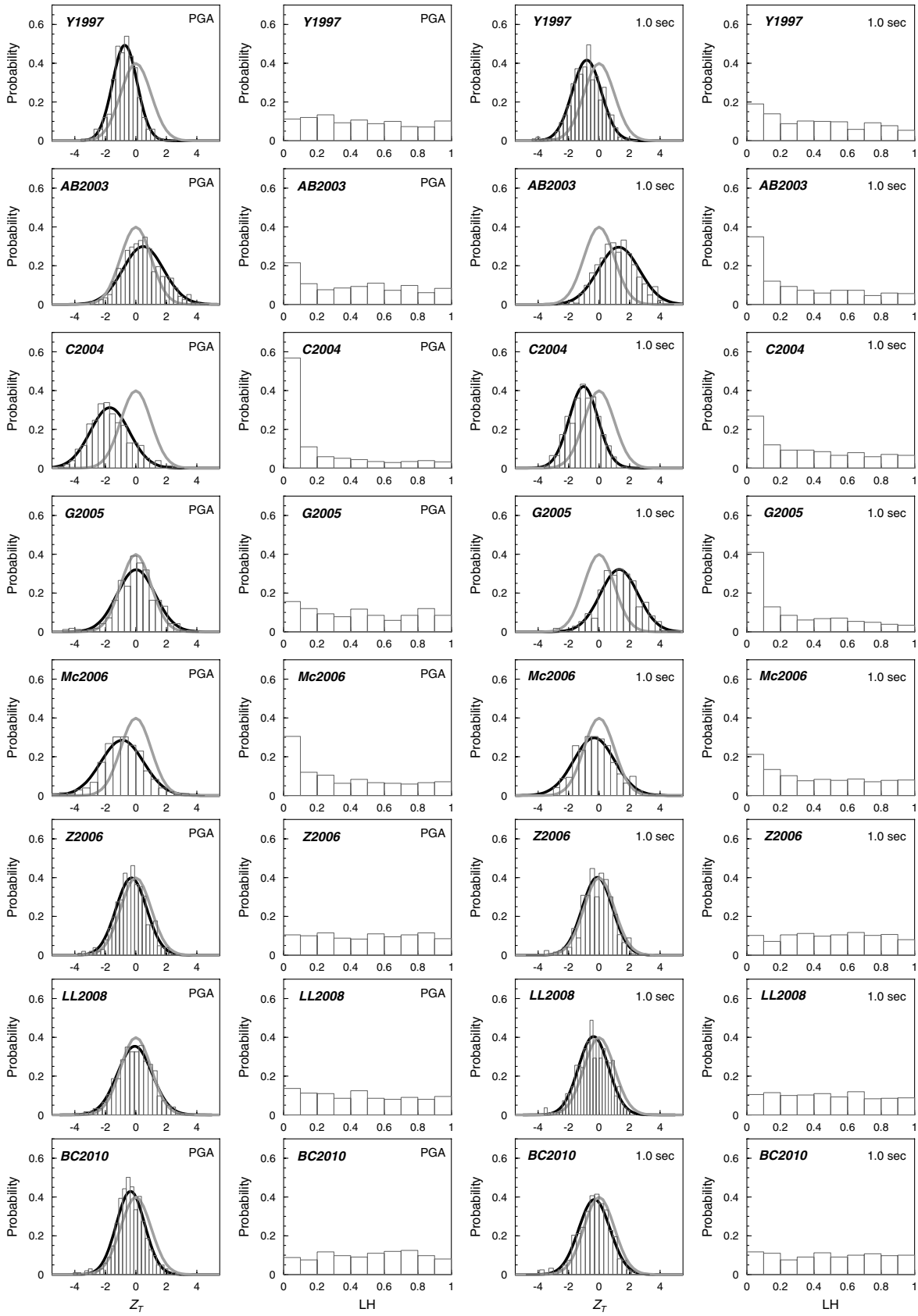

Figure 9. Distributions of the normalized total model residuals (Z_T) and associated likelihood values (LH_T) for the selected equations at PGA and 1 s, tested against the CAM intraslab dataset. The plots of the normalized model residuals also include the standard normal distribution (gray solid line) and the normal distribution fitted to the residuals (black solid line).

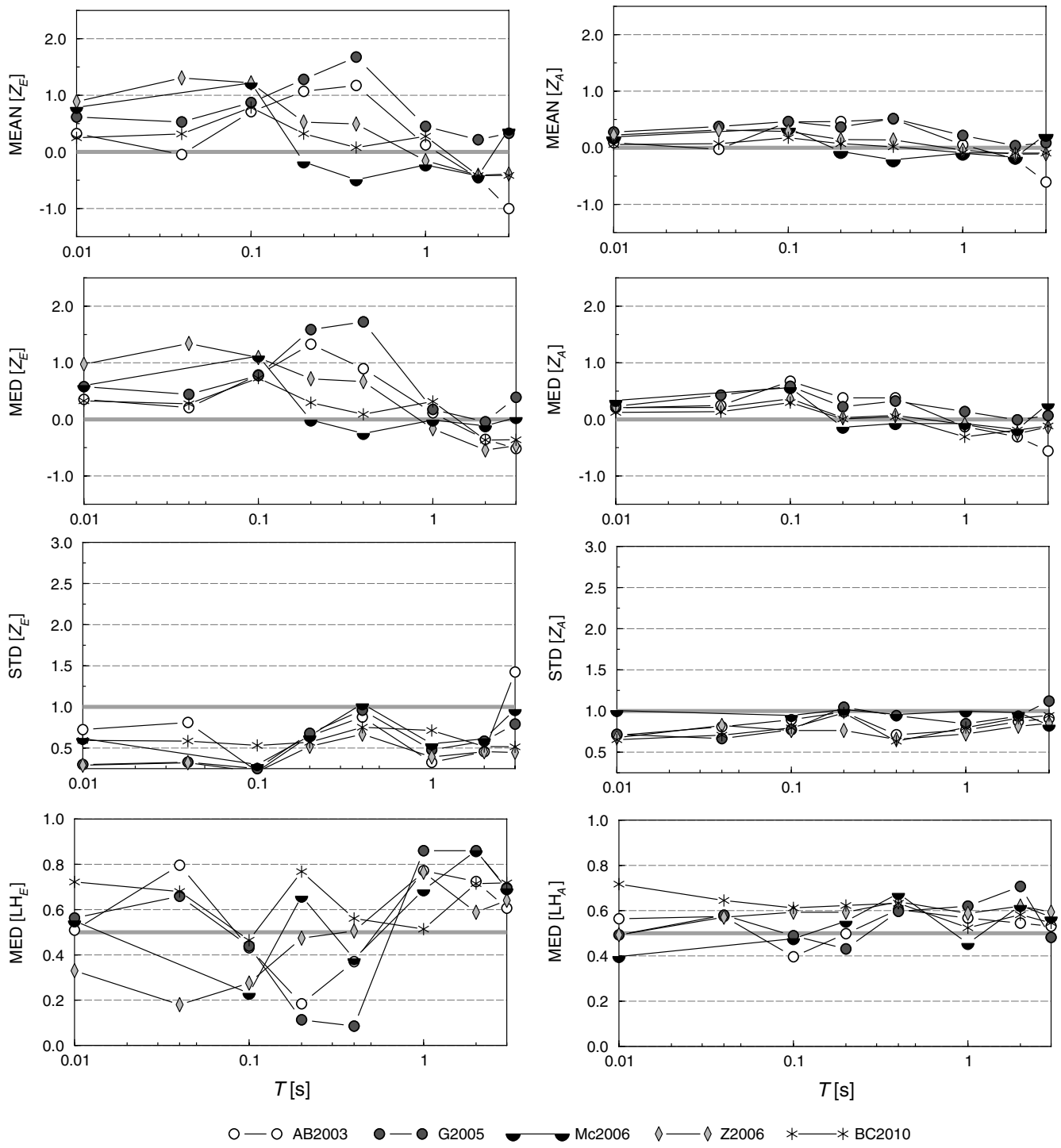

Figure 10. Goodness-of-fit measures associated with the normalized interevent (Z_E) and intraevent (Z_A) model residuals for selected intraslab equations, tested against the SAM dataset. The thick gray lines show the target values: MEAN$[Z_X]$ and MED$[Z_X] = 0$; STD$[Z_X] = 1.0$; MED$[\mathrm{LH}_X] = 0.5$. Note that the Y1997, C2004 and LL2008 models are not included (see text for details).

that in some cases the equations have been tested beyond their strict limits of applicability. Figures 6 and 10 suggest that, while the selected models appear to match reasonably well with the observed data from both interface and intraslab events in Peru–Chile on the basis of the intraevent residuals, the interevent residuals indicate a systematic underprediction at periods less than 1 s. A similar behavior was observed for the Central American datasets (Figs. 7 and 11), with the selected equations performing better on the basis of intraevent residuals, although the interevent residuals for the CAM intraslab dataset do not show a clear pattern of systematic underprediction.

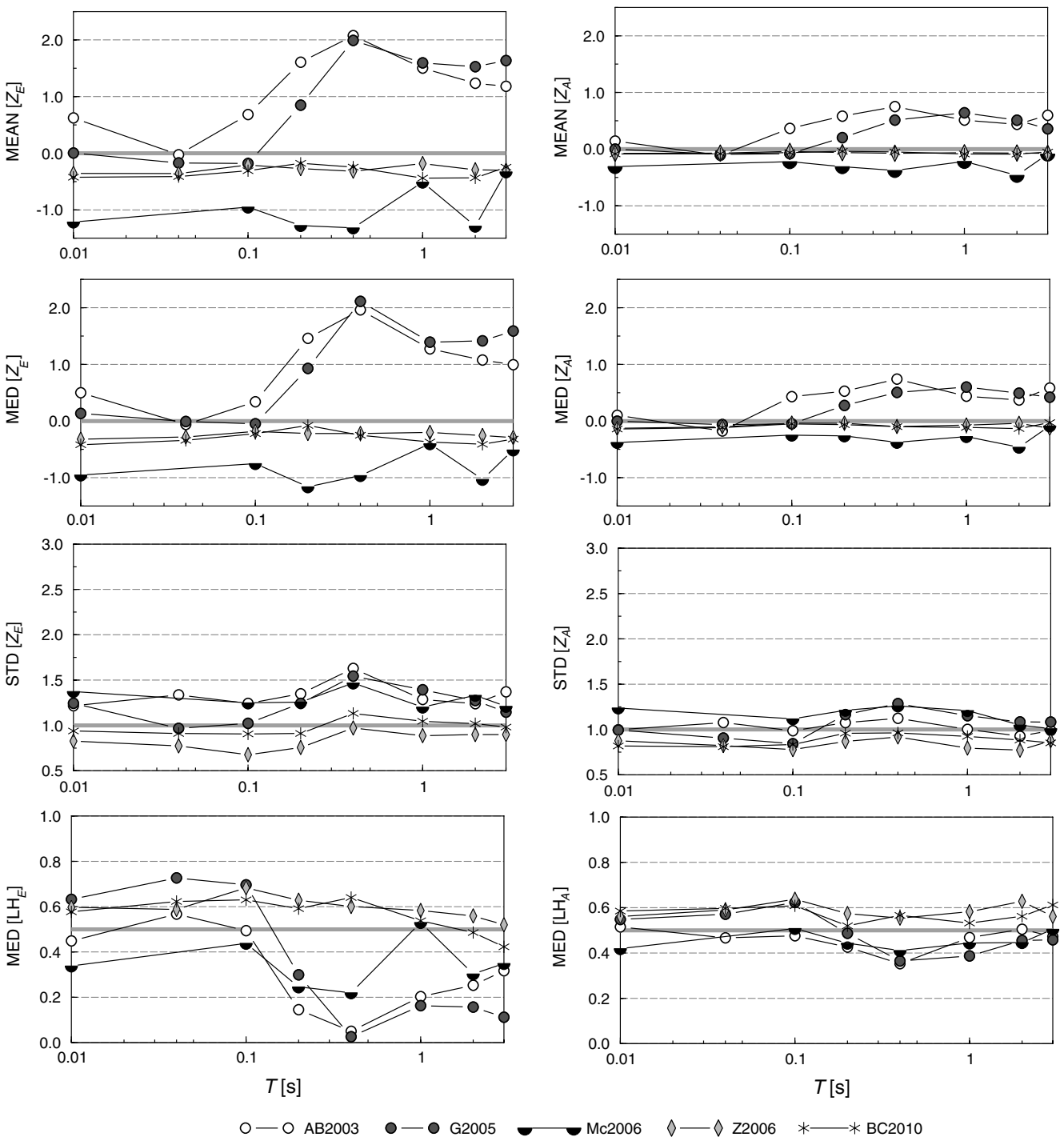

Figure 11. Goodness-of-fit measures associated with the normalized interevent (Z_E) and intraevent (Z_A) model residuals for selected intraslab equations, tested against the CAM dataset. The thick gray lines show the target values: MEAN $[Z_X]$ and MED $[Z_X] = 0$; STD $[Z_X] = 1.0$; MED $[\mathrm{LH}_X] = 0.5$. Note that the Y1997, C2004 and LL2008 models are not included (see text for details).

Overall, the results of this study indicate that the BC2010 and Z2006 models, which are largely based on extensive datasets from Japan and Taiwan, are suitable for ground-motion prediction in both the Peru–Chile and Central American subduction zones. While this could be interpreted in terms of regional similarities, it may also suggest that other factors, such as data quality and robustness of the model, can have a larger impact on the quality of the predictions than the geographic provenance of the data. To this end, one important issue to investigate is the question of regional differences between ground motions from different subduction-zone regions, which have been a topic of much debate for ground motions from shallow crustal earthquakes (e.g., Bommer, 2006; Douglas, 2007; Akkar and Çağnan, 2010). For

subduction-zone earthquakes, some differences in ground motions between regions may be expected as a result of differing degrees of coupling at the interface, geometries of the subducted plate, and material properties. Such differences have become apparent in the comparisons between observed and predicted ground motions carried out within the present study, although there may be several plausible explanations for any such ground-motion differences.

In order to investigate whether the results presented in this study suggest regional differences of the ground-motion amplitudes between the SAM and CAM subduction zones, the mean interevent model residuals for these regions and for both interface and intraslab events were examined, as shown in Figure 12. They show apparent differences in scaling of ground-motion amplitudes with magnitude between these two regions for both interface and intraslab events. For events of similar size, the ground-motion amplitudes observed in the South American region are generally larger than those observed in Central America, suggesting that a magnitude scaling effect may be responsible for these

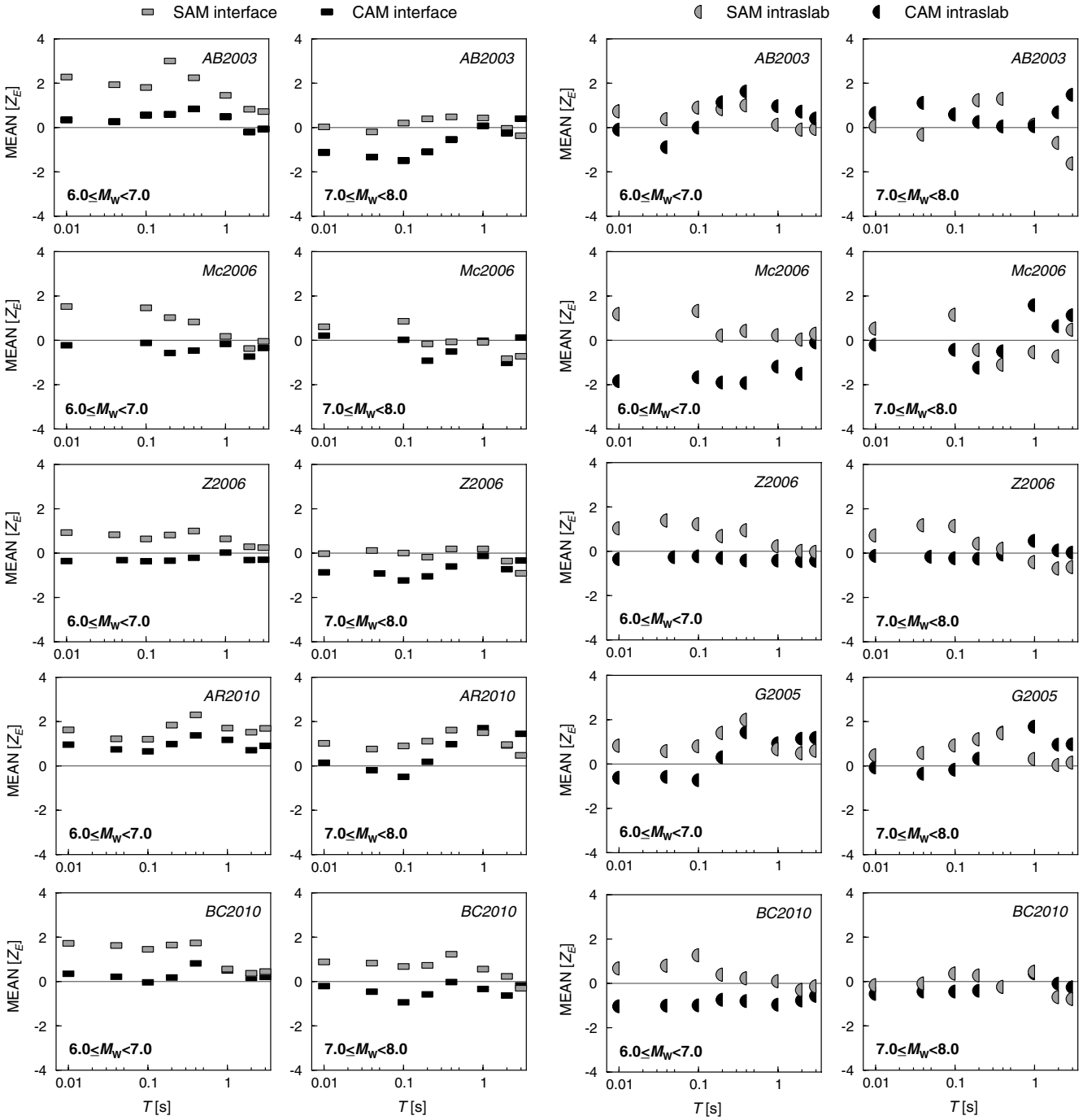

Figure 12. Mean normalized interevent model residuals MEAN [Z_E] between the selected models and the SAM and CAM datasets across the spectral periods and for three magnitude bins.

differences. There have been relatively few studies to date exploring regional differences in ground-motions from subduction-zone earthquakes (e.g. Atkinson and Boore, 2003; Atkinson and Casey, 2003; Atkinson and Macias, 2009; García and Wald, 2010). Atkinson and Boore (2003) and Atkinson and Casey (2003) attributed observed differences between ground motions from Japan and Cascadia to regional differences in site response, and Atkinson and Macias (2009) also suggest differences in terms of attenuation characteristics between Mexico and Cascadia.

The differences observed between the CAM and SAM datasets in this study may simply reflect the fact that the magnitude ranges covered by the two regional datasets for interface events are very different, with the CAM data concentrated at smaller magnitudes and all recordings associated with magnitudes greater than 7.5 coming from Chile and Peru. However, this needs to be considered against the fact that the residuals of a given model have been tested for interface events from both datasets in consistent magnitude bins. Moreover, it should also be noted that discrepancies have been observed between the SAM dataset and the GMPEs derived from datasets covering a comparable magnitude range, which might indicate that there are genuine regional differences.

The analyses have also revealed a number of issues pertaining to the modeling of the physical processes involved in the generation and propagation of strong ground motions: the scaling of ground-motion amplitudes with magnitude needs to be investigated in greater detail in order to obtain magnitude scaling functions that can be used over a wider range of magnitudes than the domain of validity of current equations. This issue has become evident in the comparisons between the selected interface models and the CAM dataset. In particular, the AB2003 interface model largely underpredicts the small magnitude data, although this should not limit its applicability to the Central American region, given the good performance of the model in the magnitude ranges that are relevant to hazard calculations. We note that mismatches between observations and predictions of GMPEs extrapolated to magnitudes lower than their intended range of applicability are commonly encountered in shallow crustal environments (Bommer *et al.*, 2007). It is also interesting to note the poor fit of the Mexican AR2010 model to the Central American data. This could suggest regional differences in ground motion between these regions, which correspond to different subduction zones (in Central America, the Cocos plate is subducting under the Caribbean plate, whereas in Mexico it is below the North American plate). This behavior is not likely to be associated to response of soil sites, which are not specifically modeled by the AR2010 equation, because the mean intraevent model residuals are close to zero.

Another important observation from this study is that the global interface model of AB2003 tends to underestimate the variability of the observed interface data from Peru and Chile, which has implications for seismic hazard estimates in these regions. It is interesting to note that the AB2003 and G2005 models, developed specifically for intraslab conditions, adequately predict the larger high-frequency motions produced by intraslab events but underestimate amplitudes at 0.2 and 0.4 s. A similar pattern was observed for the CAM intraslab data, which tend to be underpredicted by the AB2003 and G2005 models at periods longer than 0.1 s.

Conclusion

The present paper has discussed the extent to which current ground-motion models for subduction-zone earthquakes may be applied to the South and Central America subduction zones. The selection of appropriate models for ground-motion prediction in a particular region is one of the major sources of epistemic uncertainty in seismic hazard analysis, which is usually addressed by combining several models within a logic-tree framework (Bommer *et al.*, 2005). The results presented herein allow the selection of ground-motion models for the Peru–Chile and Central American regions to be informed in a rational manner. They suggest that the Y1997, AB2003, Z2006, and BC2010 models can be used to estimate the ground-motion levels due to interface events in the Peru–Chile region, although given their variable performance across the spectral ordinates, the relative weights assigned to these models may differ depending on the engineering application. Indeed, while defining an overall ranking of the models reflecting the performance of a model across all response periods seems appealing, such a definition is necessarily dependent on the specific needs of the user, because different applications may place greater emphasis on different period ranges or earthquake types. Combining the rankings into a single performance index could therefore obscure the actual relative performance of the predictive equations in certain circumstances. Instead, readers are advised to focus on the rankings at the periods of interest for the specific application considered when assessing the relative performance of the models and assigning logic-tree weights. The intraslab equations of BC2010, Mc2006, and Z2006 can be used to populate logic-tree branches in the Peru–Chile region, in view of their consistently good performance across the spectral ordinates. For the Central American region, the Z2006 and LL2008 interface equations were found to perform well, followed by the Y1997, Mc2006, and BC2010 models. The analyses of the CAM intraslab data have also shown that the Z2006, LL2008, and BC2010 intraslab models perform best, followed by the Y1997 model.

The results also highlight the evolution of ground-motion prediction for subduction-zone environments, despite the fact that it has, to date, received considerably less attention than its counterpart for shallow crustal tectonic settings. Any hazard study carried out for the South and Central American regions prior to 2005 would have had limited models to populate the GMPE branches of a logic-tree. The analyses presented in the current study suggest that recently derived global models now provide a workable solution to this problem.

Data and Resources

The full results for the SAM and CAM datasets in terms of the goodness-of-fit measures MEAN $[Z_X]$, MED $[Z_X]$, STD $[Z_X]$, and MED $[LH_X]$, where the subscript X reflects the component of variability considered (T, total; E, interevent; A, intraevent) are available as an electronic supplement to this paper. The strong-motion data and associated metadata used to assess the performance of subduction models are presented in Arango, Strasser, Bommer, Boroschek, *et al.* (2011) and Arango, Strasser, Bommer, Hernandez, *et al.* (2011).

Acknowledgments

The doctoral research of the first author, on which this paper is based, has been partially funded by the Alβan Programme of the European Union under scholarship E05D053967CO and the COLFUTURO scholarship-loan programme; their financial support is gratefully acknowledged. The authors would also like to thank Norman Abrahamson for providing the coefficients for the BC Hydro (2010) model, and David Boore, Gail Atkinson, and Daniel García for their help with issues concerning their predictive equations. The paper has greatly benefited from thoughtful reviews by Stéphane Drouet and an anonymous reviewer. Finally, we would like to thank David Edwards, Ahmer Wadee, and Catherine O'Sullivan for their assistance in the preparation and upload of the electronic supplement.

References

Akkar, S., and Z. Çağnan (2010). A local ground-motion predictive model for Turkey, and its comparison with other regional and global ground-motion models, *Bull. Seismol. Soc. Am.* **100,** 2978–2995.

Al Atik, L., N. Abrahamson, J. J. Bommer, F. Scherbaum, F. Cotton, and N. Kuehn (2010). The variability of ground-motion prediction models and its components, *Seismol. Res. Lett.* **81,** 794–801.

Alfaro, C. S., A. S. Kiremidjian, and R. A. White (1990). Seismic zoning and ground motion parameters for El Salvador, Report No. 93. The John A. Blume Earthquake Engineering Center, Stanford University, Palo Alto, California.

Arango, M. C., F. O. Strasser, J. J. Bommer, R. Boroschek, and D. Comte (2011). Strong ground motions from the Peru-Chile subduction zone, *J. Seismol.* **15,** 19–41.

Arango, M. C., F. O. Strasser, J. J. Bommer, D. A. Hernandez, and J. M. Cepeda (2011). A strong-motion database from the Central American subduction zone, *J. Seismol.* **15,** 261–294.

Arroyo, D., D. García, M. Ordaz, M. A. Mora, and S. K. Singh (2010). Strong ground-motion relations for Mexican interplate earthquakes, *J. Seismol.* **14,** 769–785.

Atkinson, G. M., and D. M. Boore (1997). Stochastic point-source modeling of ground motions in the Cascadia region, *Seismol. Res. Lett.* **68,** 74–85.

Atkinson, G. M., and D. M. Boore (2003). Empirical ground-motion relations for subduction-zone earthquakes and their application to Cascadia and other regions, *Bull. Seismol. Soc. Am.* **93,** 1703–1729.

Atkinson, G. M., and D. M. Boore (2008). Erratum to empirical ground-motion relations for subduction-zone earthquakes and their application to Cascadia and other regions, *Bull. Seismol. Soc. Am.* **98,** 2567–2569.

Atkinson, G., and R. Casey (2003). A comparative study of the 2001 Nisqually, Washington and Geiyo, Japan in-slab earthquakes, *Bull. Seismol. Soc. Am.* **93,** 1823–1831.

Atkinson, G. M., and M. Macias (2009). Predicted ground motions for great interface earthquakes in the Cascadia subduction zone, *Bull. Seismol. Soc. Am.* **99,** 1552–1578.

BC Hydro (2010). PSHA for Western Canada: Volume 3-Ground Motion Models, BC Hydro Report E658, July, BC Hydro, Vancouver, Canada.

Beyer, K., and J. J. Bommer (2006). Relationships between median values and aleatory variabilities for different definitions of the horizontal component of motion, *Bull. Seismol. Soc. Am.* **96,** 377–389.

Bindi, D, L. Luzi, F. Pacor, G. Franceschina, and R. R. Castro (2006). Ground-motion predictions from empirical attenuation relationships versus recorded data: The case of the 1997–1998 Umbria-Marche, central Italy, strong-motion data set, *Bull. Seismol. Soc. Am.* **96,** 984–100.

Bommer, J. J. (2006). Empirical estimation of ground motion: Advances and issues, *Proc. 3rd Int. Symp. on the Effects of Surface Geology on Seismic Motion*, Paper No. KN8, Grenoble, France, 29 August–1 September 2006.

Bommer, J. J., J. Douglas, F. Scherbaum, F. Cotton, H. Bungum, and D. Fäh (2010). On the selection of ground-motion prediction equations for seismic hazard analysis, *Seismol. Res. Lett.* **81,** 783–793.

Bommer, J. J., D. A. Hernández, J. A. Navarrete, and W. M. Salazar (1996). Seismic hazard assessments for El Salvador, *Geofís. Int.* **35,** 227–244.

Bommer, J. J., F. Scherbaum, H. Bungum, F. Cotton, and F. Sabetta (2005). On the use of logic trees for ground-motion prediction equations in seismic hazard analysis, *Bull. Seismol. Soc. Am.* **95,** 377–389.

Bommer, J. J., P. Stafford, J. E. Alarcón, and S. Akkar (2007). The influence of magnitude range on empirical ground-motion prediction, *Bull. Seismol. Soc. Am.* **97,** 2152–2170.

Boore, D. M., W. B. Joyner, and T. E. Fumal (1993). Estimation of response spectra and peak accelerations from western North American earthquakes: An interim report, *U.S. Geol. Surv. Open-File Rept. 93-509*, 72 pp.

Boore, D. M., A. Skarlatoudis, B. Margaris, C. Papazachos, and C. Ventouzi (2009). Along-arc and back-arc attenuation, site response, and source spectrum for the intermediate-depth 8 January 2006 *M* 6.7 Kythera, Greece, earthquake, *Bull. Seismol. Soc. Am.* **99,** 2410–2434.

Cepeda, J. M., M. B. Benito, and E. A. Burgos (2004). Strong-motion characteristics of January and February 2001 earthquakes in El Salvador, in Rose, W. I., J. J. Bommer, D. L. López, M. J. Carr, and J. J. Major (Editors), *Special Paper 375: Natural Hazards in El Salvador* Geological Society of America, Boulder, Colorado, 405–421.

Climent, A., W. Taylor, M. Ciudad Real, W. Strauch, M. Villagran, A. Dahle, and H. Bungum (1994). Spectral strong motion attenuation in Central America, *NORSAR Technical Report No. 2–17*, 46 pp.

Contreras, V. A. (2009). Curvas de atenuación espectrales para sismos chilenos, *Graduate Degree Dissertation*, Civil Engineering Department, University of Chile, 215 pp. (in Spanish).

Cotton, F., F. Scherbaum, J. J. Bommer, and H. Bungum (2006). Criteria for selecting and adjusting ground-motion models for specific target regions: Application to central Europe and rock sites, *J. Seismol.* **10,** 137–156.

Crouse, C. B. (1991). Ground-motion attenuation equations for earthquakes on the Cascadia subduction zones, *Earthq. Spectra* **7,** 201–236.

Crouse, C. B., Y. K. Vyas, and B. A. Schell (1988). Ground motion from subduction-zone earthquakes, *Bull. Seismol. Soc. Am.* **78,** 1–25.

Douglas, J. (2007). On the regional dependence of earthquake response spectra, *ISET J. Earthq. Technol.* **44,** 71–99.

Douglas, J., and R. Mohais (2009). Comparing predicted and observed ground motions from subduction earthquakes in the Lesser Antilles, *J. Seismol.* **13,** 577–587.

Douglas, J., D. Bertil, A. Roullé, P. Dominique, and P. Jousset (2006). A preliminary investigation of strong-motion data from the French Antilles, *J. Seismol.* **10,** 271–299.

Drouet, S., F. Scherbaum, F. Cotton, and A. Souriau (2007). Selection and ranking of ground motion models for seismic hazard analysis in the Pyrenees, *J. Seismol.* **11,** 87–100.

García, D., and D. J. Wald (2010). Do strong ground motions in subduction zones show regional dependence? Abstract No. S51B-1933, *American Geophysical Union Fall Meeting 2010*, San Francisco, California.

García, D., S. K. Singh, M. Herráiz, M. Ordaz, and J. F. Pacheco (2005). Inslab earthquakes of Central Mexico: Peak ground-motion parameters and response spectra, *Bull. Seismol. Soc. Am.* **95,** 2272–2282.

Gregor, N., W. Silva, I. Wong, and R. Youngs (2002). Ground motion attenuation relationships for Cascadia subduction zone megathrust earthquakes based on a stochastic finite-fault model, *Bull. Seismol. Soc. Am.* **92,** 1923–1932.

Gupta, I. D. (2010). Response spectral attenuation relations for in-slab earthquakes in Indo-Burmese subduction zone, *Soil Dynam. Earthq. Eng.* **30,** 368–377.

Hintersberger, E., F. Scherbaum, and S. Hainzl (2007). Update of likelihood-based ground-motion model selection for seismic hazard in western central Europe, *Bull. Earthq. Eng.* **5,** 1–16.

Kanno, T., A. Narita, N. Morikawa, H. Fujiwara, and F. Yoshimitsu (2006). A new attenuation relation for strong ground motion in Japan based on recorded data, *Bull. Seismol. Soc. Am.* **96,** 879–897.

Lin, P., and C. Lee (2008). Ground-motion attenuation relationships for subduction-zone earthquakes in northeastern Taiwan, *Bull. Seismol. Soc. Am.* **98,** 220–240.

Macias, M., G. Atkinson, and D. Motazedian (2008). Ground motion attenuation, source and site effects for the September 26, 2003, *M* 8.1 Tokachi-Oki earthquake sequence, *Bull. Seismol. Soc. Am.* **98,** 1947–1963.

Martín, A. (1990). Hacia una nueva regionalización y cálculo del peligro sísmico en Chile. *Civil Engineering Degree Dissertation*, Department of Physical Sciences and Mathematics, University of Chile, Santiago, Chile (in Spanish).

McVerry, G., J. Zhao, N. Abrahamson, and P. Somerville (2006). New Zealand acceleration response spectrum attenuation relations for crustal and subduction zone earthquakes, *Bull. New Zeal. Natl. Soc. Earthq. Eng.* **39,** 1–58.

Medina, M. (1998). Análisis comparativo de métodos de regresión de atenuación de aceleración máxima, *Civil Engineering Degree Dissertation*, Department of Physical Sciences and Mathematics, University of Chile, Santiago, Chile (in Spanish).

Megawati, K., and T. C. Pan (2010). Ground-motion attenuation relationship for the Sumatran megathrust earthquakes, *Earthq. Eng. Struct. Dynam.* **39,** 827–845.

Megawati, K, T. C. Pan, and K. Koketsu (2005). Response spectral attenuation relationships for Sumatran-subduction earthquakes and the seismic hazard implications to Singapore and Kuala Lumpur, *Soil Dynam. Earthq. Eng.* **25,**11–25.

National Earthquake Hazards Reduction Program (NEHRP; 1997). Recommended provisions for seismic regulations for new buildings and other structures, *FEMA Report 303*, U.S. Federal Emergency Management Agency, Washington, D.C., 366 pp.

Ruiz, S, and G. Saragoni (2005). Attenuation equations for subduction-zone earthquakes in Chile considering two seismogenic mechanisms and site effects, Paper No. A01-15, *Proc., IX Jornadas Chilenas de Sismología e Ingeniería Antisísmica*, Concepción, Chile, 16–19 November 2005 (in Spanish).

Saragoni, G. R., M. Astroza, and S. Ruiz (2004). Comparative study of subduction earthquake ground motion of north, central and south America, Paper No. 104, *Proc. 13th World Conf. on Earthquake Engineering*, Vancouver, Canada, 1–6 August 2004.

Scherbaum, F., F. Cotton, and P. Smit (2004). On the use of response spectral-reference data for the selection and ranking of ground-motion models for seismic-hazard analysis in regions of moderate seismicity: The case of rock motion, *Bull. Seismol. Soc. Am.* **94,** 2164–2185.

Schmidt, V., A. Dahle, and H. Bungum (1997). Costa Rican spectral strong motion attenuation, *Technical Rept. NORSAR, Norway, 1997, Reduction of Natural Disasters in Central America Earthquake Preparedness and Hazard Mitigation Phase II: 1996–2000, Part 2*, 45 pp.

Singh, S. K., A. Iglesias, D. García, J. F. Pacheco, and M. Ordaz (2007). *Q* of *Lg* waves in the Central Mexican volcanic belt, *Bull. Seismol. Soc. Am.* **97,** 1259–1266.

Stafford, P. J., F. O. Strasser, and J. J. Bommer (2008). An evaluation of the applicability of the NGA models to ground-motion prediction in the Euro-Mediterranean region, *Bull. Earthq. Eng.* **6,** 149–177.

Strasser, F. O., M. C. Arango, and J. J. Bommer (2010). Scaling of the source dimensions of interface and intraslab subduction-zone earthquakes with moment magnitude, *Seismol. Res. Lett.* **81,** 941–950.

Takahashi, T., A. Asano, T. Saiki, H. Okada, K. Irikura, J. X. Zhao, J. Zhang, H. K. Thio, P. G. Somerville, Y. Fukushima, and Y. Fukushima (2004). Attenuation models for response spectra derived from Japanese strong-motion records accounting for tectonic source types, Paper No. 1271, *Proc. 13th World Conf. on Earthquake Engineering*, Vancouver, Canada, 1–6 August 2004.

Youngs, R. R., S. J. Chiou, W. J. Silva, and J. R. Humphrey (1997). Strong ground motion attenuation relationships for subduction zone earthquakes, *Seismol. Res. Lett.* **68,** 58–77.

Zhao, J. X., J. Zhang, A. Asano, Y. Ohno, T. Oouchi, T. Takahashi, H. Ogawa, K. Irikura, H. K. Thio, P. G. Somerville, and Y. Fukushima (2006). Attenuation relations of strong ground motion in Japan using site classification based on predominant period, *Bull. Seismol. Soc. Am.* **96,** 898–913.

Department of Civil and Environmental Engineering
Imperial College London
London
SW7 2AZ
United Kingdom
(M.C.A., J.J.B.)

Seismology Unit
Council for Geoscience
Private Bag X112
Pretoria
0001
South Africa
fstrasser@geoscience.org.za
(F.O.S.)

Natural Hazards Division & International Centre for Geohazards
Norwegian Geotechnical Institute (NGI)
Sognsveien 72
0855 Oslo
Norway
(J.M.C.)

Department of Civil Engineering
University of Chile
Blanco Encalada 2002
Santiago, Chile
(R.B.)

Gerencia de Geología
Dirección General del Observatorio Ambiental
Ministerio de Medio Ambiente y Recursos Naturales
Km 5 1/2, Carretera a Santa Tecla, Av. Las Mercedes
San Salvador, El Salvador
(D.A.H.)

Seismology Department
Geophysical Institute of Peru
Calle Badajoz 169
Urb Mayorazgo IV Etapa
Ate, Lima
Peru
(H.T.)

Manuscript received 14 March 2011